1994ApJ...423..248L

THE ASTROPHYSICAL JOURNAL, 423:248–265, 1994 March 1
© 1994. The American Astronomical Society. All rights reserved. Printed in U.S.A.

THE HORIZONTAL-BRANCH STARS IN GLOBULAR CLUSTERS. II. THE SECOND PARAMETER PHENOMENON

YOUNG-WOOK LEE
Yonsei University Observatory, Seoul 120-749, Korea; and Department of Astronomy, Yale University
AND
PIERRE DEMARQUE AND ROBERT ZINN
Department of Astronomy, Yale University, New Haven, CT 06511
Received 1993 February 12; accepted 1993 September 2

ABSTRACT

Using synthetic horizontal-branch models, we have investigated the origin of the systematic variation in horizontal-branch (HB) morphology with galactocentric distance (R_G) among globular clusters. The variations in He abundance, CNO abundance, and core mass required separately to explain this effect are inconsistent with either the observed properties of the RR Lyrae variables or the observed main-sequence turnoffs in the clusters. There is also no clear evidence that the trend with R_G is related to the central concentrations, central densities, or absolute magnitudes of the clusters. The variations in cluster age required to explain this effect are not in conflict with any observations. A detailed comparison of our synthetic HB calculations with pairs of clusters of very different HB morphology but similar [Fe/H] reveals reasonably good agreement between the age differences inferred from HB morphology and the main-sequence turnoff. The major source of uncertainty is the need for ad hoc hypotheses in the modeling of the HB morphologies of a few peculiar clusters (e.g., NGC 6752). Nonetheless, there is firm evidence for age variations of several gigayears (as much as ~ 5 Gyr) among the halo globular clusters. Our results support the hypothesis of Searle & Zinn that the inner halo is more uniform in age and is older in the mean than the outer halo, and we estimate this difference to be ~ 2 Gyr.

Subject headings: Galaxy: formation — globular clusters: general — stars: evolution — stars: horizontal-branch

1. INTRODUCTION

The horizontal-branch (HB) morphology of a globular cluster is in simplest terms the distribution in color of its HB stars. A red or blue HB is one where the bulk of the stars lie to the red or blue side of the RR Lyrae instability strip. HB morphology depends on metal abundance (the *first* parameter) in the sense that all metal-rich clusters (i.e., [Fe/H] > -0.8) have very red HBs, whereas metal-poor clusters have a variety of HB types, including some consisting solely of very blue HB stars. Twenty-seven years ago, van den Bergh (1967) and Sandage & Wildey (1967) showed that some metal-poor clusters of the same metal abundance have very different HB types; hence there must be a *second* parameter, in addition to metal abundance, that influences HB morphology. These early discussions suggested that the second parameter might be the abundance of He, but it was soon realized that the ratio of the abundances of C, N, and O to that of Fe, the amount of core rotation, and cluster age were equally plausible second parameters (see Faulkner 1966; Rood 1973; Renzini 1977; Demarque 1980; Rood & Seitzer 1981). Van den Bergh (1967) and Sandage & Wildey (1967) also noted that the most distant globular clusters and the dwarf spheroidal galaxies exhibit the second parameter phenomenon in extreme form, for in spite of their metal-poor compositions, they have very red HBs. Thus, the phenomenon is related to position in the Galaxy and hence also to the Galaxy's evolution. Expanding on this, Searle & Zinn (1978, hereafter SZ) showed that there is systematic variation of the strength of the second parameter with galactocentric distance (R_G) in the sense that at small distances HB morphology and [Fe/H] are closely tied to one another and with increasing distance there is more scatter in HB type and the mean HB type becomes redder at a given [Fe/H]. Substantial improvements in the quantity and quality of HB types and [Fe/H] measurements made this trend with R_G even more striking (Zinn 1980; Lee, Demarque, & Zinn 1988b; this paper). SZ argued that the most likely explanation of this effect was that cluster age was the second parameter and the trend with R_G indicated that the metal enrichment of galactic halo proceeded rapidly near its center and that the outer halo was built up over a several billion year period by the merging of protogalactic fragments. This view has received considerable support in recent years from the measurement of significant age differences between clusters of the same metal abundance but different HB morphologies (Lee et al. 1988b; Demarque et al. 1988; Gratton & Ortolani 1988; Bolte 1989; Stetson et al. 1989; Green & Norris 1990; Buonanno et al. 1990, 1993; VandenBerg, Bolte, & Stetson 1990; Sarajedini & Demarque 1990; Da Costa, Armandroff, & Norris 1992) and from the measurements of the abundances and kinematics of halo objects, which show that [Fe/H] and kinematics are uncorrelated (Carney, Latham, & Land 1990; Norris & Ryan 1991 and references therein), as predicted by SZ. However, only a small number of clusters have been dated to sufficiently high precision to test the hypothesis that the second parameter is age, and there is some doubt that the detected age differences are consistent with the HB morphologies of the clusters. If they are not, this would suggest that age cannot be the sole second parameter.

The high-precision photometry of globular clusters in recent years has shown that some HBs have complex structures. For example, pronounced gaps occur in the color distributions of

© American Astronomical Society • Provided by the NASA Astrophysics Data System

1994ApJ...423..248L

the HB stars in NGC 6752 (Cannon 1981; Buonanno et al. 1986b) and M15 (Buonanno, Corsi, & Fusi Pecci 1985). These clusters and a few others display the "blue tail phenomenon," where the HB extends to very blue colors and faint absolute V magnitude (M_V). The color distribution of the HB stars in NGC 2808 is markedly bimodal, characterized by a both a red clump and a blue HB with few stars in between (see Harris 1975; Byun & Lee 1991). In a few other clusters, there is some evidence of radial variations in HB morphology (e.g., Buonanno et al. 1991; Bailyn et al. 1992). Recent papers by Fusi Pecci et al. (1992) and Buonanno (1993) have shown that the total length of the HB and the length of the blue tail are correlated with cluster density and concentration, in the sense that the clusters having the highest central densities and highest concentrations have on average longer HB's and blue tails. In addition, the radial dropoff in density within a cluster is suspected to be the origin of the radial variations in HB morphology (Buonanno et al. 1991; Djorgovski & Piotto 1992). Thus, there are good reasons to include central density and concentration in the list of candidate second parameters.

In this paper, we investigate the origin of the systematic variation in HB morphology with galactocentric distance by comparing synthetic models of the HB with the HBs in real clusters. We consider separately the hypotheses that the parameter controlling this variation is the abundance of He, the CNO/Fe ratio, and core rotation, and for each of them, we find serious conflicts with one or more of the observed characteristics of the HB, the RR Lyrae variables, or the main-sequence (M-S) turnoff. The hypothesis that cluster age is responsible is consistent with these data, and we show that the differences in age between a few famous pairs of clusters, as inferred from their M-S turnoffs, are sufficient to account for their differences in HB morphology, without added hypotheses. We show that variation in HB morphology with R_G cannot be due to cluster density or central concentration alone. We concur with previous investigators, however, that some HB anomalies, e.g., blue tails, defy explanation by the age hypothesis for the second parameter and that cluster density/concentration is an attractive alternative for them. We are led to the conclusion that cluster age is the major variable causing the variation in HB morphology with R_G, and we briefly discuss the implications that this has for the evolution of the Galaxy.

2. MODELS OF THE HORIZONTAL-BRANCH

Following closely the methods of our previous investigations (e.g., Lee et al. 1988b, Lee, Demarque & Zinn 1990 [hereafter Paper I]), we have calculated synthetic HB models for a variety of chemical compositions and ages, and under two assumptions regarding the mass loss on the red giant branch. We assumed a truncated Gaussian distribution for the masses of the HB stars, as did Rood (1973) in his pioneering study. Unlike most other HB syntheses, ours were constructed from post–zero age horizontal-branch (ZAHB) evolutionary tracks that extended to the point of complete exhaustion of helium in the core. They included, therefore, the last 5%–10% of the HB lifetime, which is particularly important for modeling the Oosterhoff group II clusters (see Paper I). The initial ZAHB models had helium core masses appropriate for their compositions, and the evolutionary tracks (Lee & Demarque 1990) covered fine grids in composition and mass (Δ[Fe/H] ≤ 0.3, $\Delta Y = 0.03$, $\Delta M = 0.02$–$0.04\ M_\odot$). Evolutionary tracks including recent improvements in opacities and other physics are in excellent agreement with this grid (Dorman, Lee, & VandenBerg 1991; Yi, Lee, & Demarque 1993).

Before considering the possible second parameters, we show in Figure 1 the effects that variable metal abundance (Z) have

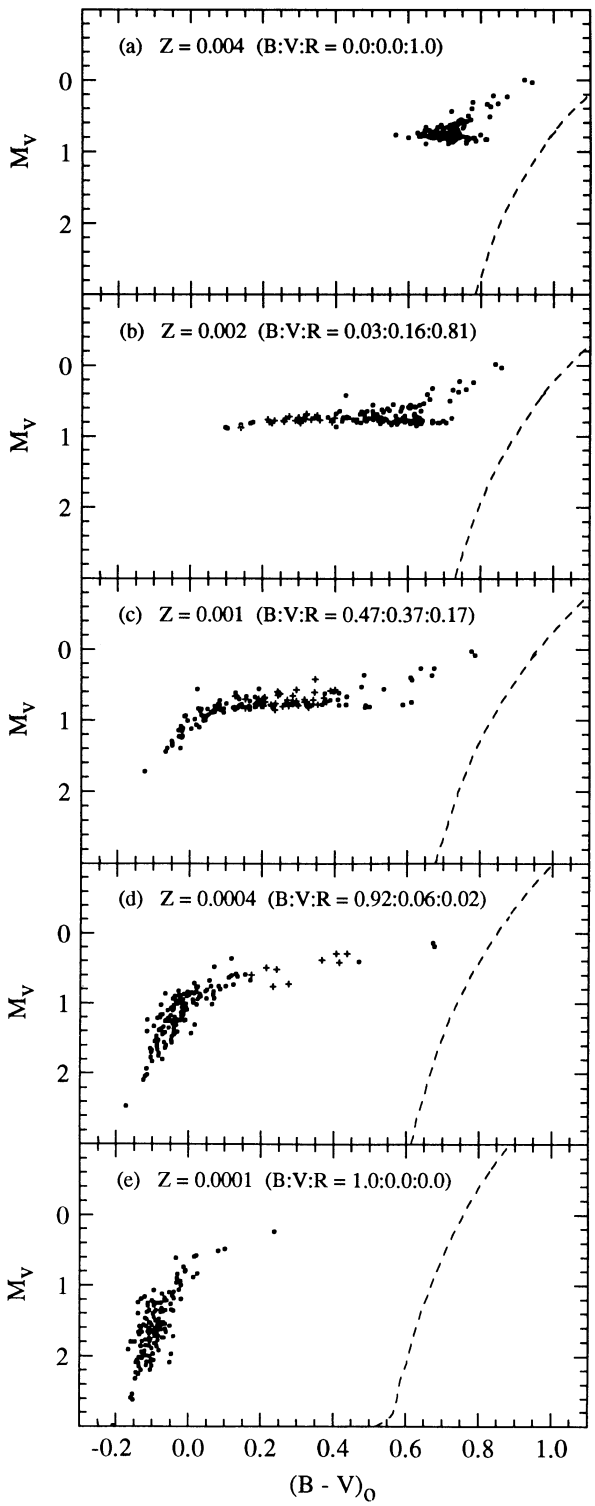


FIG. 1.—(*a–e*) The effect of metallicity on the morphology of the HB. Cluster age (13 Gyr) Y_{HB} (~ 0.22), and ΔM ($0.223\ M_\odot$) are fixed. The loci of the giant branch are from the Revised Yale Isochrones (Green et al. 1987). Observational errors ($\sigma_V \approx 0.02$; $\sigma_{B-V} \approx 0.03$) are included in the HB simulations.

© American Astronomical Society • Provided by the NASA Astrophysics Data System

1994ApJ...423..248L

on the appearance of the HB in the *C-M* diagram. For these synthetic HB calculations, the mean mass-loss ($\Delta M = 0.223\ M_\odot$), HB helium abundance ($Y_{HB} \approx 0.22$), and cluster age (13 Gyr) have been fixed, while the metal abundance varies from $Z = 0.004$ to $Z = 0.0001$. The amount of mass dispersion on the HB (σ_M) is assumed to be $\sim 0.02\ M_\odot$ (see Lee 1990) for all synthetic HB calculations described in this paper, unless otherwise specified. Figure 1 illustrates the well-known result that the HB becomes redder with increasing Z. This is mainly a consequence of the larger opacities in the envelopes of the metal-rich stars (see, e.g., Sweigart 1987). Since the mass of a red giant at the helium flash (M_{RG}) increases with increasing Z (see Green et al. 1987; VandenBerg & Bell 1985), the metal-rich HB stars are also more massive than the metal-poor stars if the amount of mass-loss does not vary. This also contributes to the redward shift of the HB with increasing Z, although to a smaller degree than the increase in opacity.

The effect of cluster age on the morphology of the HB is shown in Figure 2. The other parameters, Y_{HB} (~ 0.22), Z (0.001), and mass loss ($\Delta M = 0.223\ M_\odot$), are held constant. Age differences of several billion years produce dramatic changes in the morphology of the HB in the sense that the older clusters have bluer HBs. This is due to the fact that the mean mass of the HB stars ($\langle M_{HB} \rangle$) is decreasing as M_{RG} decreases with increasing age (see Green et al. 1987; VandenBerg 1983). If we adopt the Reimers' (1977) mass-loss relation, the mass-loss rate increases slightly as M_{RG} decreases (with increasing age). This produces a stronger dependence of HB type on age than that obtained with fixed mass-loss assumption (see Fig. 3). In our simulations, we have used Renzini's (1977) equation (6.17), which is an analytic expression for Reimers' (1977) mass-loss relation, with the value of $\eta = 0.63$, which yields $\Delta M = 0.223\ M_\odot$ for Age = 13 Gyr and $Z = 0.001$.

The effect of envelope helium abundance is shown next in Figure 4. The other parameters ($Z = 0.001$, age = 11 Gyr, and $\Delta M = 0.223\ M_\odot$) are fixed while Y_{HB} increases from ~ 0.22 to ~ 0.25. For the same age and metal abundance, helium-rich

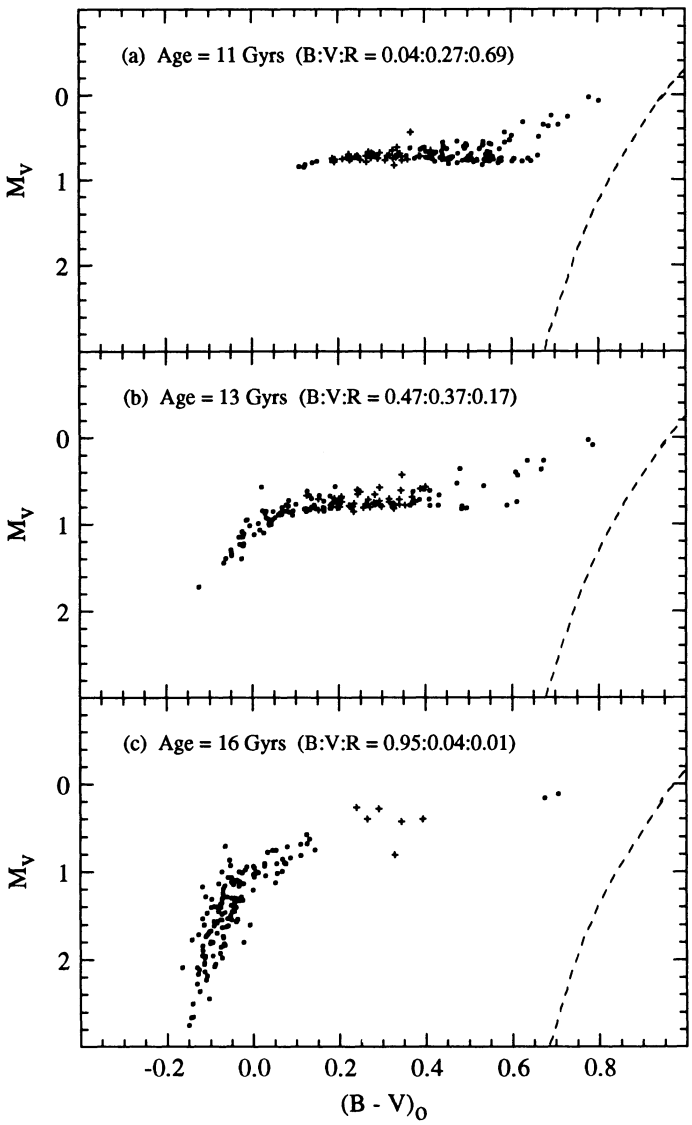


FIG. 2.—(*a–c*) The effect of cluster age on the morphology of the HB. Y_{HB} (~ 0.22), Z (0.001), and ΔM ($0.223\ M_\odot$) are fixed.

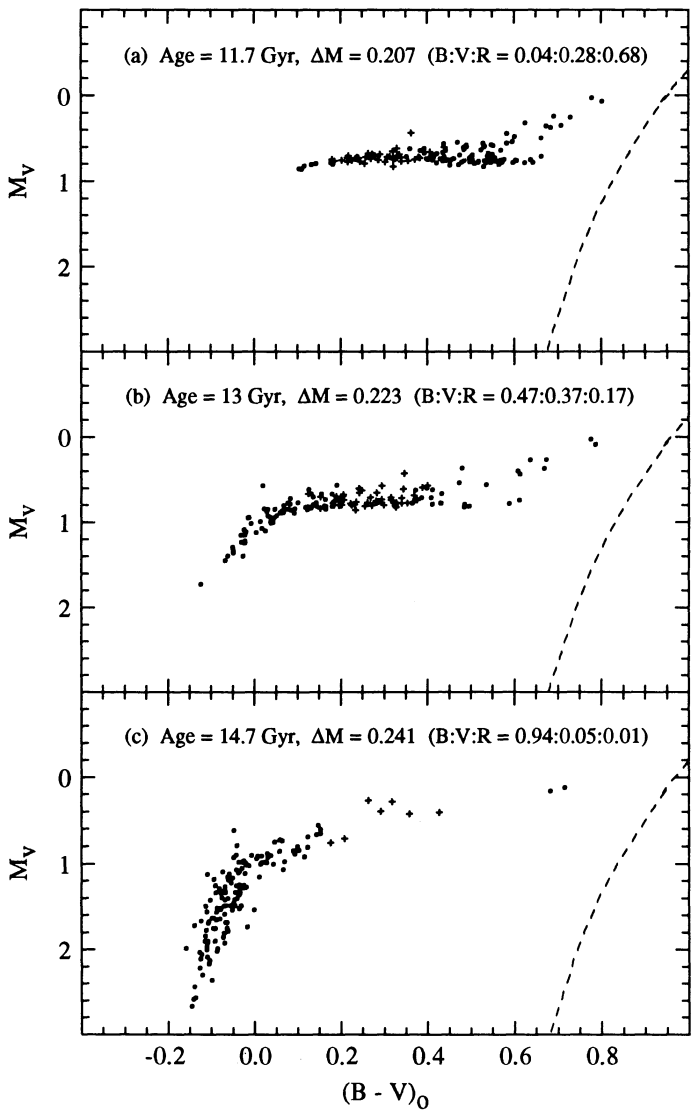


FIG. 3.—(*a–c*) Same as Fig. 2, but with the Reimers' (1977) mass-loss relation. Note that the HB morphology incorporating the results of Reimers show a stronger age dependence than that of fixed mass-loss assumption (see Fig. 2).

© American Astronomical Society • Provided by the NASA Astrophysics Data System

1994ApJ...423..248L

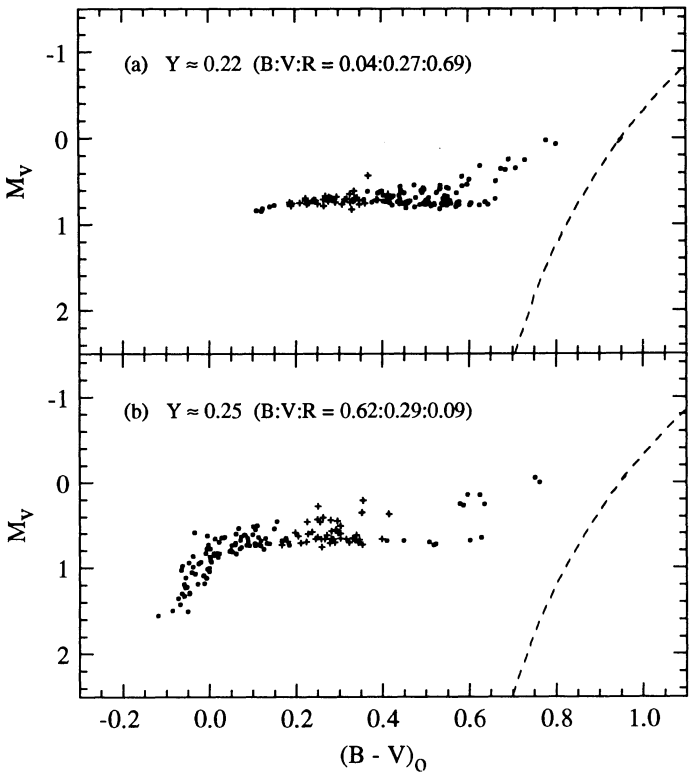


FIG. 4.—(*a–b*) The effect of envelope helium abundance on the morphology of the HB. Cluster age (11 Gyr), Z (0.001), and ΔM (0.223 $M_\odot$) are fixed.

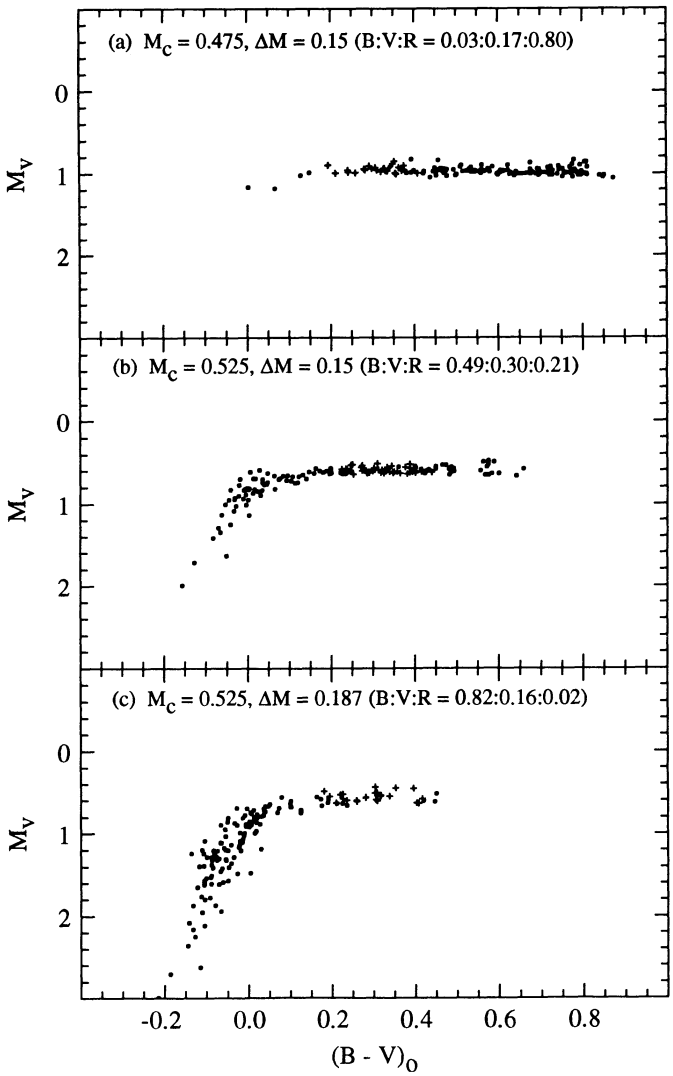


FIG. 5.—(*a–c*) The possible effects of core rotation (ω) on the morphology of the HB. Panels (*a*) and (*b*) show the effect of increasing M_c by 0.05 $M_\odot$ due to an increase in ω by 3.75×10^{-4} rad s^{-1}. Panel (*c*) shows the effect of increasing M_c and the mass loss simultaneously (see text).

HB stars have smaller total masses than do less He-rich stars, which shifts their ZAHB positions to the blue. In addition, the post-ZAHB evolutionary tracks of the He rich stars have longer blueward loops (see Sweigart 1987; Lee & Demarque 1990). Consequently, as Y_{HB} increases, the HB shifts markedly to the blue (see Fig. 4).

The appearance of the HB is also suspected to be sensitive to the core rotation (ω). From simple models that assume angular momentum conservation in the stellar core, Mengel & Gross (1976) suggested three principal effects which internal rotation might have on the evolution of low-mass stars: (1) the helium core mass on the ZAHB increases as a consequence of the delayed ignition of the helium core flash at the tip of the red-giant branch, (2) the luminosity at the tip of the red-giant branch (L_{fl}) is higher, and (3) the turnoff ages are increased for a given total mass (i.e., M_{RG} is increased for a given age). The first two effects favor bluer HB, because the HB gets bluer as M_c increases (Sweigart & Gross 1976), and also because ΔM increases with increasing L_{fl}, if one adopts the Reimers' (1977) mass-loss relationship (see Renzini 1977). The last effect, however, favors redder HB, for the mean mass of the HB stars, $\langle M_{HB} \rangle$, increases as M_{RG} increases. To simulate these possible effects of core rotation on the appearance of the HB, we have used Sweigart & Gross (1976) tracks for HB stars of different core masses (M_c). Results are shown in Figure 5. The only changes between Figures 5*a* and 5*b* are increases in M_c from 0.475 to 0.525 $M_\odot$ (effect 1) and in M_{RG} from 0.819 to 0.838 $M_\odot$ (effect 3) due to an increase in ω from 0.0 to 3.75×10^{-4} rad s^{-1} (these values are estimated from Mengel & Gross 1976). The blueward shift with increasing ω is thus due to the fact that the effect 1 overwhelms effect 3. If ΔM increases as L_{fl} increases with increasing ω (effect 2), the blueward shift is even larger (see Fig. 5*c*). To estimate the effect of L_{fl} on ΔM, we have again used Renzini's (1977) analytical expression for Reimers' (1977) mass-loss relation.

Finally, since the CNO abundance governs the energy generation and opacity of HB stars, it affects the structure of an HB model (see Dorman et al. 1991; Sweigart, Renzini, & Tornambé 1987). The synthetic HB models in Figure 6, based on recent HB evolutionary tracks with and without oxygen enhancement (Dorman et al. 1991), simulate this effect. One can see in Figure 6 that the morphology of HB gets redder as CNO abundance increases. The calculations of red giant branch evolution with a CNO enhancement (Rood 1981) indicate that L_{fl} may increase slightly with increasing [CNO/Fe] for a given age; hence it is possible that ΔM also increases somewhat with increasing [CNO/Fe] if one adopts the Reimers' mass-loss relationship. If this is correct, then Renzini's (1977) equation for Reimers' (1977) mass-loss relation suggests that slightly larger (by $\sim$10%) difference in

© American Astronomical Society • Provided by the NASA Astrophysics Data System

1994ApJ...423..248L

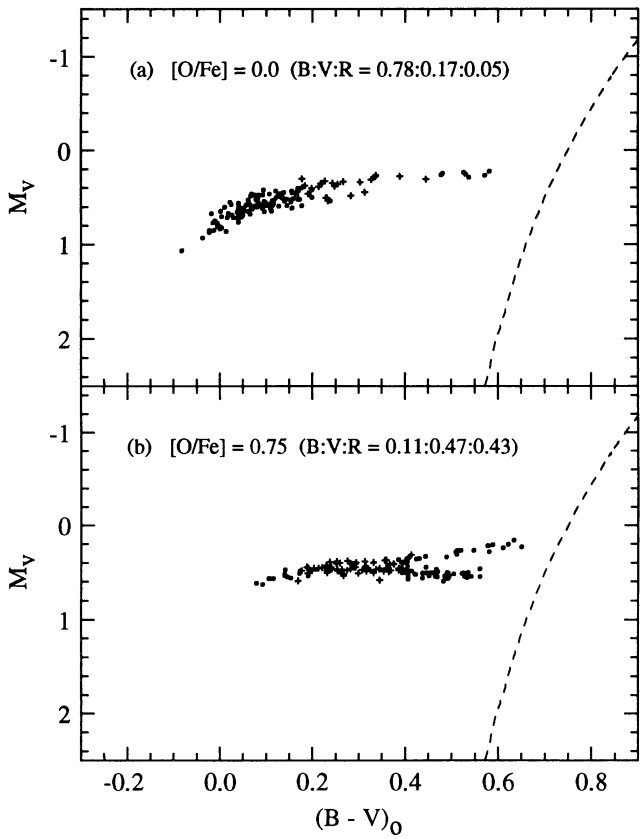


FIG. 6.—(*a–b*) The effect of [O/Fe] on the morphology of the HB. Other parameters are fixed (age = 10 Gyr, [Fe/H] = −2.26, $Y_{HB} = 0.245$, and $\Delta M = 0.15\ M_\odot$).

[CNO/Fe] may be required for the same change in the HB morphology.

The synthetic HB models shown in Figures 1–6 are but a few of an extensive series of calculations that cover wide ranges in each of the variables Z, age, ω (M_c), and O/Fe. They are compared with real clusters through the use of the following classifiction scheme for HB morphology.

3. CLASSIFICATION OF HORIZONTAL-BRANCH MORPHOLOGY

To classify the morphology of the HB, we have used the quantity, $(B-R)/(B+V+R)$, where B, V, and R are the numbers of *blue* HB stars, RR Lyrae *variables*, and *red* HB stars, respectively. $(B-R)/(B+V+R)$ ranges from -1, for clusters that possess only a red HB (e.g., 47 Tuc), to $+1$ for those containing a purely blue HB (e.g., NGC 6752). Clusters that possess nearly equal numbers of red and blue HB stars (e.g., M3) are assigned the values of $\sim$0.0. Because the RR Lyrae variables are included, this index distinguishes between two clusters with red (or blue) HB stars, but one with and one without RR Lyrae's.

Our synthetic HB calculations indicate that $(B-R)/(B+V+R)$ depends mostly on the location of the peak of the color distribution of the HB stars and only slightly on the dispersion in color of the HB stars. Fusi Pecci et al. (1992) came to the same conclusion from observational data. By using $(B-R)/(B+V+R)$ as classification index, we are focusing on the origin of the differences in peak location among clusters of the same [Fe/H]. It is these differences that exhibit a systematic variation with R_G in the Galaxy, which is the subject of this paper. The origin of the differences in color dispersion from cluster to cluster, for which $(B-R)/(B+V+R)$ provides little information, is also an important question, as Fusi Pecci et al. (1992) and Buonanno (1993) have emphasized. It will be addressed by us in a later paper.

To calculate $(B-R)/(B+V+R)$, we have counted the values of B, V, and R for 83 globular clusters with reasonably well studied C-M diagrams. These values are listed in Table 1, along with the resulting value of $(B-R)/(B+V+R)$. These numbers pertain only to the area of the sky included in the listed photometric catalog and are not, therefore, the total numbers of such stars in each cluster. When the number of variables within the area selected for the construction of C-M diagram is not given in the source of the C-M diagram, it was estimated from Hogg's (1973) catalog of variable stars in globular clusters. In some clusters, there is some ambiguity concerning whether certain stars are field stars or HB stars; consequently their values of B, V, and/or R are marked with colons in Table 1. There are few clusters whose HB lie predominantly to the blue of the instability strip with some RR Lyrae variables, but the existing photometry barely reaches the level of the HB. The values of B and $(B-R)/(B+V+R)$ in Table 1 are thus uncertain for these clusters (NGC 4590, 6402, and 6656) and represent only lower limits of true values. The uncertainties (σ) of the HB types were estimated by constructing $\sim$50 synthetic HB calculations (see Paper I; Lee 1990) with sample sizes, chemical compositions, and HB types similar to the observed HBs. The standard deviations derived from these calculations provide estimates of the uncertainty due to the random distribution of stars along the evolutionary tracks. Because of the incompleteness of the sample, and because of the contamination of the C-M diagram by field stars, the real values of σ should be substantially larger than these lower limits. Consequently, the estimated values of σ from the synthetic HB calculations have been multiplied by factors ($\sim$2) that we think provide better estimates of the uncertainty from all sources as judged by an empirical estimate based on the multiple studies of several clusters in Table 1. Table 1 lists the values of [Fe/H] on the Zinn & West (1984, hereafter ZW) metallicity scale from Zinn (1985), unless a more recent measurement was available from Armandroff & Zinn (1988), Da Costa & Seitzer (1989), Suntzeff, Olszewski, & Stetson (1985), Armandroff & Da Costa (1991), Suntzeff, Kraft, & Kinman (1988), Da Costa et al. (1992), and Armandroff, Da Costa, & Zinn (1992). The 1 σ errors in [Fe/H] indicate the precisions with which the clusters are ranked on the ZW scale, and they do not include therefore the uncertanty in the scale. The small values of $\sigma_{[Fe/H]}$ for many of the clusters in Table 1 are a consequence of averaging the results from several different techniques which are in excellent agreement. Also listed in Table 1 are the galactocentric distances (R_G) of the clusters and the sources of the C-M diagrams. In our calculations of R_G, we have followed the methodology of Zinn (1985), but adopted the new M_v(HB)–[Fe/H] relation predicted by our synthetic HB calculations ($M_v^{RR} = 0.19$ [Fe/H] + 1.00; see eq. [5] of Paper I) and 8 kpc for the Sun's galactocentric distance ($R_\odot$). None of our conclusions hinge on the choice of this M_v^{RR}–[Fe/H] relationship. For several clusters, the C-M diagrams referenced in Table 1 have yielded better values of M_v(HB) than were available to Zinn (1985). Omega Centauri has been excluded from the sample of clusters considered here because of its

© American Astronomical Society • Provided by the NASA Astrophysics Data System

1994ApJ...423..248L

TABLE 1

HORIZONTAL-BRANCH TYPES

NGC	Name	B	V	R	(B-R)/(B+V+R)		[Fe/H]		R (Kpc)	CM Diagram
104	47 Tuc	0	0	77	-1.00	±0.03	-0.71	±0.08	7.3	Hesser *et al.* 1987
288		99	1	2	0.95	0.08	-1.40	0.12	11.2	Buonanno *et al.* 1984
362		3	4	71	-0.87	0.08	-1.28	0.07	9.0	Harris 1982
1261		3	9	38	-0.70	0.10	-1.29	0.09	16.9	Alcaino 1979b
1851		29	11	63	-0.33	0.08	-1.29	0.09	15.8	Stetson 1981
1904	M79	31	4	0	0.89	0.16	-1.68	0.09	18.4	Stetson & Harris 1977
2298		14	1	0	0.93	0.24	-1.81	0.11	14.6	Alcaino & Liller 1986
2419		92	12	3:	0.83	0.14	-2.02	0.07	98.8	Racine & Harris 1975
2808		60	2:	203	-0.54	0.06	-1.37	0.09	10.8	Byun & Lee 1991
3201		65	60	51	0.08	0.06	-1.56	0.12	8.8	Lee 1977b
4147		41	14	7	0.55	0.14	-1.80	0.14	19.1	Sandage & Walker 1955
4372		76:	0	0	1.00	0.10	-2.08	0.15	7.0	Hartwick & Hesser 1973
4590	M68	>22	18	4:	>0.41	>0.18	-2.09	0.11	9.7	Alcaino 1977
4833		167	8	0	0.95	0.06	-1.86	0.09	6.8	Menzies 1972
5024	M53	139	31	6	0.76	0.10	-2.04	0.08	18.9	Cuffey 1965
5053		32	7	5	0.61	0.18	-2.41	0.12	16.5	Light 1988
5272	M3	75	95	56	0.08	0.04	-1.66	0.06	11.6	Buonanno *et al.* 1986a
5286		32	3	0	0.91	0.18	-1.79	0.11	7.0	Harris *et al.* 1976
5466		56	17	4	0.68	0.14	-2.22	0.36	16.2	Buonanno *et al.* 1985
5694		30	0	0	1.00	0.15	-1.91	0.11	26.9	Ortolani & Gratton 1990
5824		43	5	2:	0.82	0.14	-1.87	0.15	25.7	Cannon *et al.* 1990
5897		101	4	3	0.91	0.10	-1.68	0.11	7.4	Sarajedini 1992a
5904	M5	92	40	32	0.37	0.06	-1.40	0.06	6.1	Buonanno *et al.* 1981
5927		0	0	60:	-1.00	0.04	-0.31	0.09	4.5	Menzies 1974
5986		53	3	0	0.95	0.14	-1.67	0.12	4.3	Harris *et al.* 1976
6093	M80	34	3	0	0.92	0.16	-1.64	0.12	3.0	Harris & Racine 1974
6101		74	5	4:	0.84	0.16	-1.81	0.15	10.5	Sarajedini & Da Costa 1991
6121	M4	52	38	63	-0.07	0.10	-1.28	0.10	6.3	Lee 1977a
6144		>22	0	0	1.00	0.16	-1.75	0.15	2.9	Alcaino 1980
6171	M107	3	15	71	-0.76	0.08	-0.99	0.06	3.5	Dickens & Rolland 1972
6205	M13	110	3	0	0.97	0.08	-1.65	0.06	8.3	Philip *et al.* 1976
6218	M12	70:.	0	3:	0.92	0.10	-1.61	0.12	4.3	Racine 1971
6229		45	14	24	0.25	0.14	-1.54	0.10	28.1	Carney et al. 1991
6235		27	3	0	0.90	0.16	-1.40	0.15	2.5	Liller 1980a
6254	M10	63	0	2:	0.94	0.10	-1.60	0.08	4.7	Harris *et al.* 1976
6266	M62	63:	15:	32:	0.28	0.20	-1.29	0.15	2.0	Caloi *et al.* 1987
6293		37	4	0	0.90	0.18	-1.92	0.15	1.4	Janes & Heasley 1991
6316		0	0	60:	-1.00	0.04	-0.55	0.15	4.2	Armandroff 1988
6333	M9	75:	5:	3:	0.87	0.16	-1.78	0.15	1.7	Janes & Heasley 1991
6341	M92	121	10	3	0.88	0.08	-2.24	0.08	9.2	Buonanno *et al.* 1985
6342		0	0	30:	-1.00	0.04	-0.66	0.15	1.7	Armandroff 1988
6352		0	0	38	-1.00	0.04	-0.51	0.08	3.7	Hartwick & Hesser 1972
6362		17	4	69	-0.58	0.08	-1.08	0.09	5.0	Alcaino 1972
6366		0	1	51	-0.97	0.10	-0.85	0.10	4.8	Pike 1976
6397		76	0	3:	0.93	0.10	-1.91	0.14	6.1	Alcaino *et al.* 1987
6402	M14	>63	34	0	>0.65	>0.10	-1.39	0.13	3.7	Kogon *et al.* 1974
6496		0	0	35:	-1.00	0.04	-0.48	0.15	2.9	Armandroff 1988
6535		16:	0	0	1.00	0.20	-1.75	0.15	3.9	Liller 1980b
6539		0	0	30:	-1.00	0.04	-0.66	0.15	3.2	Armandroff 1988
6541		>15	0	0	1.00	± 0.20	-1.83	±0.15	2.7	Alcaino 1979a
6544		38:	0	0	1.00	0.14	-1.56	0.15	5.7	Alcaino 1983
6553		0	0	47	-1.00	0.08	-0.29	0.11	2.9	Hartwick 1975
6584		7	16:	15	-0.21	0.16	-1.54	0.15	6.3	Sarajedini 1992b
6624		0	0	22	-1.00	0.06	-0.37	0.15	1.3	Liller & Carney 1978
6626	M28	45	2	2	0.88	0.14	-1.44	0.15	2.9	Alcaino 1981
6637	M69	0	0	60:	-1.00	0.04	-0.59	0.19	1.8	Hartwick & Sandage 1968
6638		6	4	13	-0.30	0.20	-1.15	0.15	1.5	Alcaino & Liller 1983
6656	M22	>110	7:	0	>0.94	>0.10	-1.75	0.08	5.0	Cudworth 1986
6712		14	10	70	-0.60	0.08	-1.01	0.14	3.7	Sandage 1966
6723		39	20	47	-0.08	0.08	-1.09	0.14	2.6	Menzies 1974
6752		211	0	0	1.00	0.04	-1.54	0.09	5.3	Buonanno *et al.* 1986b

© American Astronomical Society • Provided by the NASA Astrophysics Data System

1994ApJ...423..248L

TABLE 1.—*Continued*

NGC	Name	B	V	R	(B-R)/(B+V+R)		[Fe/H]		R (kpc)	CM Diagram
6760		0	0	30:	-1.00	0.04	-0.52	0.15	4.9	Armandroff 1988
6779	M56	61	1	0	0.98	0.12	-1.94	0.13	9.3	Barbon 1965
6809	M55	96	3	3	0.91	0.10	-1.82	0.15	4.0	Lee 1977c
6838	M71	0	0	32:	-1.00	0.04	-0.58	0.08	6.8	Cudworth 1985
6864	M75	37	9	91	-0.39	0.08	-1.32	0.12	11.3	Harris 1975
6934		31	30	11:	0.28	0.10	-1.54	0.09	11.0	Harris & Racine 1973
6981	M72	21	14	13	0.17	0.12	-1.54	0.09	12.0	Dickens 1972
7006		46	54	64:	-0.11	0.06	-1.59	0.07	36.3	Buonanno *et al.* 1991
7078	M15	115	30	7	0.72	0.10	-2.17	0.08	10.1	Buonanno *et al.* 1985
7089	M2	80	3	0	0.96	0.10	-1.58	0.07	10.3	Harris 1975
7099	M30	62	2	3	0.88	0.12	-2.13	0.13	6.9	Alcaino & Liller 1980
7492		27	1	1	0.90	0.18	-1.51	0.3	23.4	Buonanno *et al.* 1987
...	AM-1	0	0	28:	-1.00	0.06	-1.69	0.30	113.7	Aaronson *et al.* 1984
...	Eridanus	0	0	12:	-1.00	0.10	-1.41	0.11	81.4	Da Costa 1985
...	Pal 3	0	3	14	-0.82	0.20	-1.57	0.19	89.7	Gratton & Ortolani 1984
...	Pal 4	0	0	20:	-1.00	0.06	-1.28	0.20	89.6	Christian & Heasley 1986
...	Pal 5	4	4	12	-0.40	0.20	-1.47	0.29	15.8	Sandage & Hartwick 1977
...	Pal 8	0	0	35:	-1.00	0.04	-0.48	0.16	4.7	Armandroff 1988
...	Pal 12	0	0	7:	-1.00	0.12	-1.14	0.20	14.7	Gratton & Ortolani 1988
...	Pal 14	0	0	16:	-1.00	0.08	-1.60	0.18	67.2	Harris & van den Bergh 1984
...	Pal 15	40:	0	0	1.00	0.12	-1.60	0.15	30.0	Seitzer & Carney 1990
...	Ruprecht 106	0	9:	41:	-0.82	0.15	-1.69	0.05	16.8	Buonanno *et al.* 1990

chemical inhomogeneity (see Lee 1991b for a discussion of the HB type–[Fe/H] correlation in ω Cen).

4. THE VARIATION IN HB MORPHOLOGY WITH GALACTOCENTRIC DISTANCE

The variation in HB type with R_G is shown in Figure 7, where the clusters in Table 1 have been divided by R_G into three radial zones. In this and subsequent diagrams, we do not distinguish between the metal-rich ([Fe/H] > -0.8) clusters belonging to the disk system of globular clusters and the more metal-poor halo clusters (see Zinn 1990 for a review of these cluster systems). The known sample of disk globular clusters does not extend beyond the $R_\odot$ (8 kpc); hence these clusters are confined to the first radial zone in Figure 7. The dividing line between the second and third zones was placed at 40 kpc because beyond that point the halo contains not only globular clusters but also the satellite galaxies of the Milky Way, the Magellanic Clouds and the eight dwarf spheroidal galaxies. While we will only discuss the globular clusters lying in this outermost zone, it is important to note that only one of the eight dwarf spheroidal galaxies has a blue HB. The other seven have unusually red HBs for their metal-poor compositions. Therefore, in terms of the relative frequencies of red and blue HB types, these galaxies are very similar to the globular clusters lying at comparable galactocentric distances.

The lines plotted in Figure 7 are the results of our synthetic HB calculations under the assumption that all stars suffer the same amount of mass loss on the giant branch. Each of the three lines is a constant age sequence assuming that only [Fe/H] varies from cluster to cluster. The same lines are repeated in each of the three radial zones in order to provide a backdrop against which the observational data may be compared.

The data points in Figure 7 illustrate that HB morphology varies systematically with R_G, in much the same manner as SZ concluded from their less extensive and generally less precise data set. Specifically, at a given [Fe/H], the mean HB type becomes redder and the scatter in HB type becomes larger with increasing R_G. The majority of the clusters in the inner halo ($R_G < 8$ kpc) define a very tight relationship between [Fe/H] and HB type that closely resembles the oldest of the three constant age relations. The very deviant cluster, NGC 6584, is discussed below. The clusters in the $8 \leq R_G < 40$ kpc zone exhibit considerably more scatter in HB type at a given [Fe/H] than do the clusters in the first zone. There is some semblance of a sequence, but it is shifted to lower [Fe/H] than one in the first zone. It is centered around the middle constant age line. In addition, the second zone contains several relatively metal rich clusters that have very blue HBs (e.g. NGC 288). Similar clusters are also found in the innermost zone. The majority of clusters in the $R_G \geq 40$ kpc zone have very red HB's, and they lie near the youngest of the three constant age lines.

The present sample of clusters is larger than the ones that we have considered previously (Lee & Zinn unpublished [see Zinn 1986]; Lee, Demarque, & Zinn 1988b; Lee 1989), and one consequence is that the differences in HB morphology between the three radial zones are now somewhat less distinct than before. In particular, the present sample includes NGC 6584 and Ruprecht 106, whose *C-M* diagrams have been only recently constructed. These objects appear to be out of place in Figure 7 because the HB types of NGC 6584 and R106 are more indicative of the clusters in the second and third zones, respectively, rather than ones in zones 1 and 2. For both of these clusters, a case can be made that their anomalous positions are due to the mixing between zones that must occur to some extent as the clusters orbit the galactic center.

Lin & Richer's (1992) recent analysis of the possible orbits of R106 suggests that it is currently approaching the perigalacticon point in its orbit from an apogalacticon of more than 50 kpc. Lin & Richer argue that Ruprecht 106 has been captured from the Magellanic Clouds as recently as 10^8 year ago. In which case, it provides evidence that accretion has played a role in the formation of the galactic halo, even at very recent times (see also Da Costa et al. 1992).

© American Astronomical Society • Provided by the NASA Astrophysics Data System

1994ApJ...423..248L

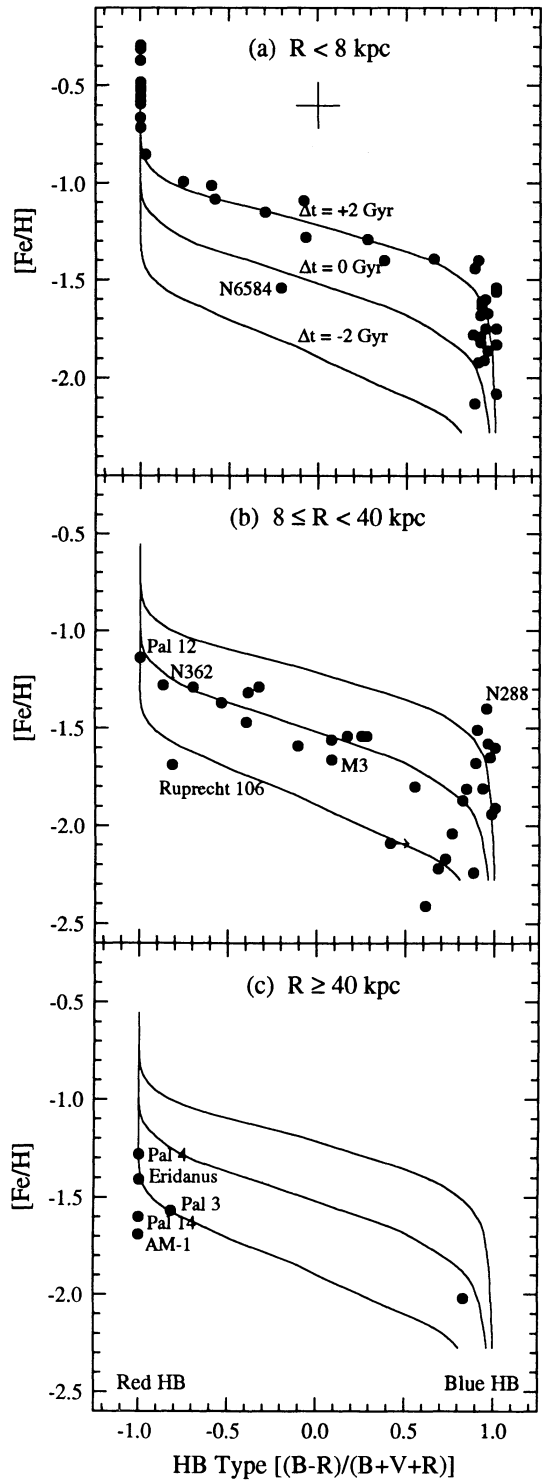


FIG. 7.—(*a–c*) The HB morphology vs. [Fe/H] relations for globular clusters in three radial zones of the Galaxy (data from Table 1). The solid lines are theoretical isochrones that were produced by the synthetic HB code (with fixed mass-loss), the upper being older. Note the systematic variation of HB type with Galactocentric distance.

NGC 6584 also appears to be far from its apogalacticon. Sarajedini (1992b) has constructed the first *C-M* diagram for this cluster, and on the basis of his determination of its V(HB), it is now possible to locate the cluster in the Galaxy with some precision. Adopting $R_\odot = 8$ kpc, the reddening listed by Zinn (1985), and the relationship given above for the absolute magnitude of the HB, we find that NGC 6584 lies on the far side of the Galactic center from the Sun, at $R_G = 6.3$ kpc. Since it lies in the direction of the Galactic center ($l = 342°$, $b = -16°$), its radial velocity with respect to the Sun ($+235 \pm 17$ km s^{-1}; Hesser et al. 1986) is nearly the same as its radial velocity with respect to the Galactic center. This large positive velocity clearly indicates that the cluster's Galactocentric distance is rapidly increasing; hence its apogalacticon is undoubtedly more than 8 kpc.

Only a small amount of orbital mixing between zones is expected because clusters on eccentric orbits spend only a small fraction of their orbital periods near their perigalacticon points (see SZ). This mixing reduces the size of radial gradient (see Harris 1990); hence the one seen in Figure 7 cannot be an artifact produced by this effect.

It is important to note that the constant age lines overlap at both the red and blue extremes of HB type. Hence, only upper or lower limits can be placed on the ages of clusters with HB types near -1 or near $+1$, respectively.

Also notice in Figure 7 that the very metal poor clusters with blue HBs (e.g., M15 and M92) do not have HB type $= +1$, in spite of the fact that age determinations based on the main-sequence turnoff consistently show that these clusters are among the oldest in the Galaxy. This inconsistency with our synthetic HB calculations is related to the nonmonotonic behavior of HB type as a function of [Fe/H], which has been discussed by Renzini (1983), Castellani (1983), Sandage (1990), and Lee (1990, 1991c). The most metal-poor clusters ([Fe/H] ≤ -2.1) contain substantial numbers of RR Lyrae variables. At [Fe/H] ~ -1.9, nearly all clusters contain few if any RR Lyrae variables, and hence their HB types are $\geq +0.9$. Above [Fe/H] ~ -1.8, one sees the second parameter at work, for their is a large range in HB type at every [Fe/H] < -1. Above [Fe/H] > -1, only red HB are observed. We suspect that the nonmonotonic behavior at low [Fe/H] is due to a decrease in the efficiency of the mass-loss mechanism with decreasing [Fe/H] (see Lee 1991b). In which case, the relatively red HBs of the very metal poor clusters are a consequence of their HB stars having larger masses than predicted by our models (either with or without the Reimers' prescription for mass loss). This inadequacy of our modeling, which may be significant only for [Fe/H] < -1.8, suggests that comparisons between clusters of different [Fe/H] should be treated with caution. Comparisons between clusters of the same [Fe/H] are, however, unaffected by our lack of knowledge of the dependency of mass-loss on [Fe/H]. The following analysis is based on comparisons between clusters of the same [Fe/H] or in a few instances between clusters more metal rich than [Fe/H] $= -1.8$ that differ in [Fe/H] by only small amounts.

5. DENSITY AND CONCENTRATION

As noted in § 1, recent investigations have suggested that the total length of the HB, L_t, the length of the blue tail, BT, and the radial variation in HB type in a few clusters may be related to the central densities of the clusters and their concentrations. However, these parameters appear to have very little, if anything, to do with the variation in HB type with R_G.

This is illustrated in Figure 8 where for the clusters in the zones $R_G < 8$ kpc and 8–40 kpc, [Fe/H], concentration [$c = \log(r_t/r_c)$], log central density, and absolute visual magnitude, M_v, are plotted against HB type (data from Table 1, Fusi

© American Astronomical Society • Provided by the NASA Astrophysics Data System

1994ApJ...423..248L

Pecci et al. 1992, and Armandroff 1989, respectively). We have included M_v because L_t and BT correlate better with it than with c and log (ρ_0) (see Figs. 14 and 15 in Fusi Pecci et al. 1992). This may mean that cluster richness, as measured by M_v, is as important as concentration and central density in the dynamical mechanism that affects L_t and BT (Fusi Pecci et al. 1992). Even in the absence of such a process, however, rich clusters are more likely to contain the relatively rare stars that populate the ends of the HB, and this alone should produce correlations between M_v and the two measures of HB length.

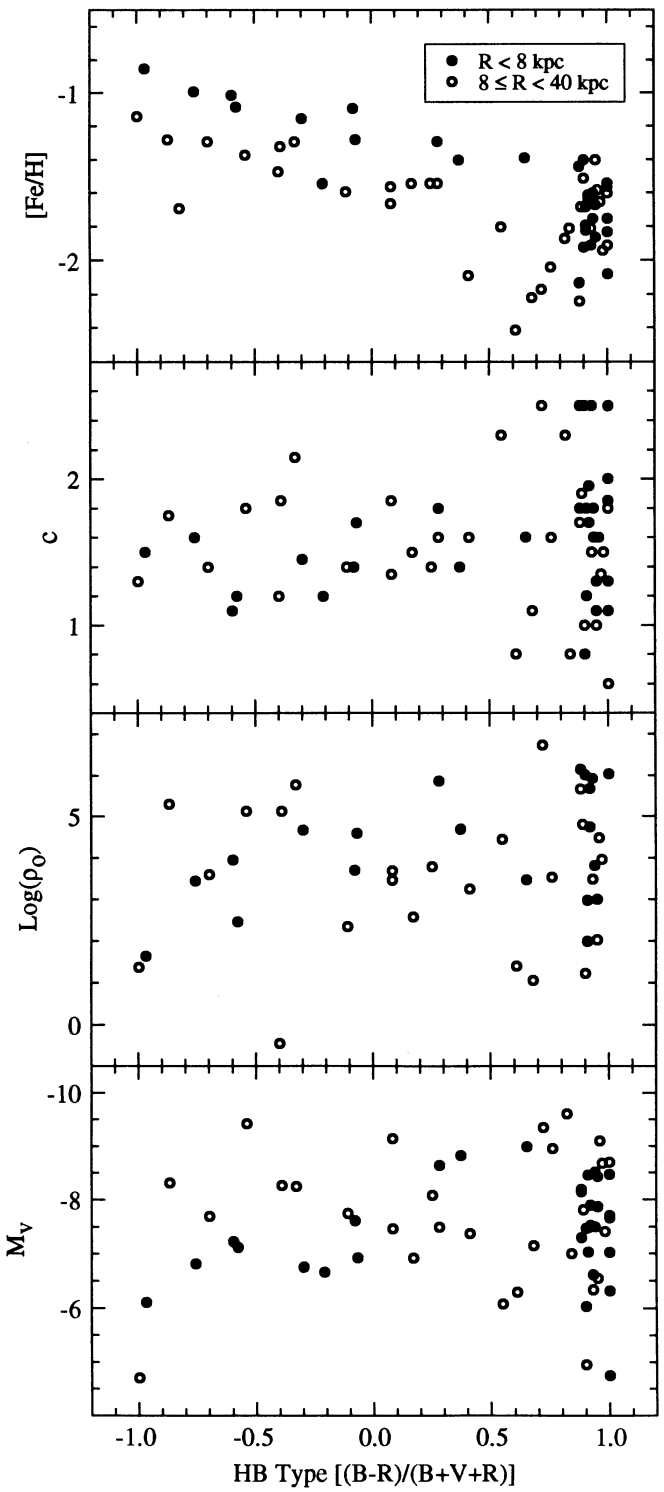


FIG. 8.—For the clusters in the zones $R_G < 8$ kpc and $8 \leq R_G < 40$ kpc, [Fe/H], concentration [c = log (r_t/r_c)], central density, and absolute visual magnitude (M_v), are plotted against HB type (see text).

Figure 8 illustrates that there is no separation in c, log (ρ_0), and M_v between the inner and outer halo clusters. It seems doubtful, therefore, that differences in these parameters can be the origin of the systematic difference in HB type at the same [Fe/H] between the inner and outer halo clusters (see the top panels of Figs. 7 and 8).

The possibility that central density and concentration influence the lengths of the HB and the blue tail and drive the radial variations in HB morphology still remains. There are, however, several counter examples. The data in Fusi Pecci et al. (1992) indicate that NGC 6229 and 6254 have large values of L_t and BT and yet these clusters have only average central densities, concentrations, and luminosities. NGC 6397 and 7099 have among the highest central densities and concentrations and yet their values of L_t and BT are very small in comparison to those of NGC 6752 and M15, which are similar to NGC 6397 and 7099 in density and concentration and bracket them in metal abundance. E. Rubenstein & C. Bailyn (1993, private communication) have recently constructed a *C-M* diagram that completely covers the central regions of NGC 6397. The HB in this diagram, which extends well below the *M-S* turnoff, is very similar in morphology to previous ones of the outer parts of the cluster (many core radii). Consequently, there is no evidence for a radial gradient in HB morphology in this extremely dense and concentrated cluster. It is not true, therefore, that central density and concentration are correlated one to one with L_t, BT, or the presence of a radial gradient in HB morphology. The peculiarities of the HB such as blue tails, gaps, and gradient may be related to central density and concentration, but apparently in a complex way.

6. CONSTRAINTS ON THE GLOBAL SECOND PARAMETER

By comparing our synthetic HB calculations with the observed HB types, we have estimated the variations in the other candidate second parameters that are needed to explain the differences between the inner ($R_G < 8$) and outer ($8 \leq R_G < 40$ kpc) zones of the halo (see Fig. 7; the anomalous clusters R106 and NGC 6584 are ignored). These estimates are listed in Table 2. Two examples of these comparisons are presented in Figure 9, where the cluster data are compared with our calculations for the cases that second parameter is either

TABLE 2

ESTIMATES OF VARIATIONS IN SECOND PARAMETERS NECESSARY TO EXPLAIN THE DIFFERENCES BETWEEN THE ZONES $R_G < 8$ kpc and $8 \leq R_G < 40$ kiloparsecs

SECOND PARAMETER	ROUGH VALUE	Δ (PARAMETER)[a] Fixed ΔM	Δ (PARAMETER)[a] Reimers' ΔM
Age	14 Gyr	2	1.5
Y	0.23	0.03	0.02
$M_c(\omega)$	0.490 $M_\odot$	0.043	0.028
[CNO/Fe]	0.4	−0.5	−0.6

[a] Δ = Inner halo ($R_G < 8$ kpc)-Outer halo ($8 \leq R_G < 40$ kpc).

© American Astronomical Society • Provided by the NASA Astrophysics Data System

1994ApJ...423..248L

age (panel *a*) or the abundance of He (panel *b*). In both panels, the solid and dashed lines are the calculations for the constant and Reimers mass-loss relations, respectively. As noted in § 2, the assumption of the Reimers relation produces a stronger dependence of HB type on age than does the assumption of uniform mass loss.

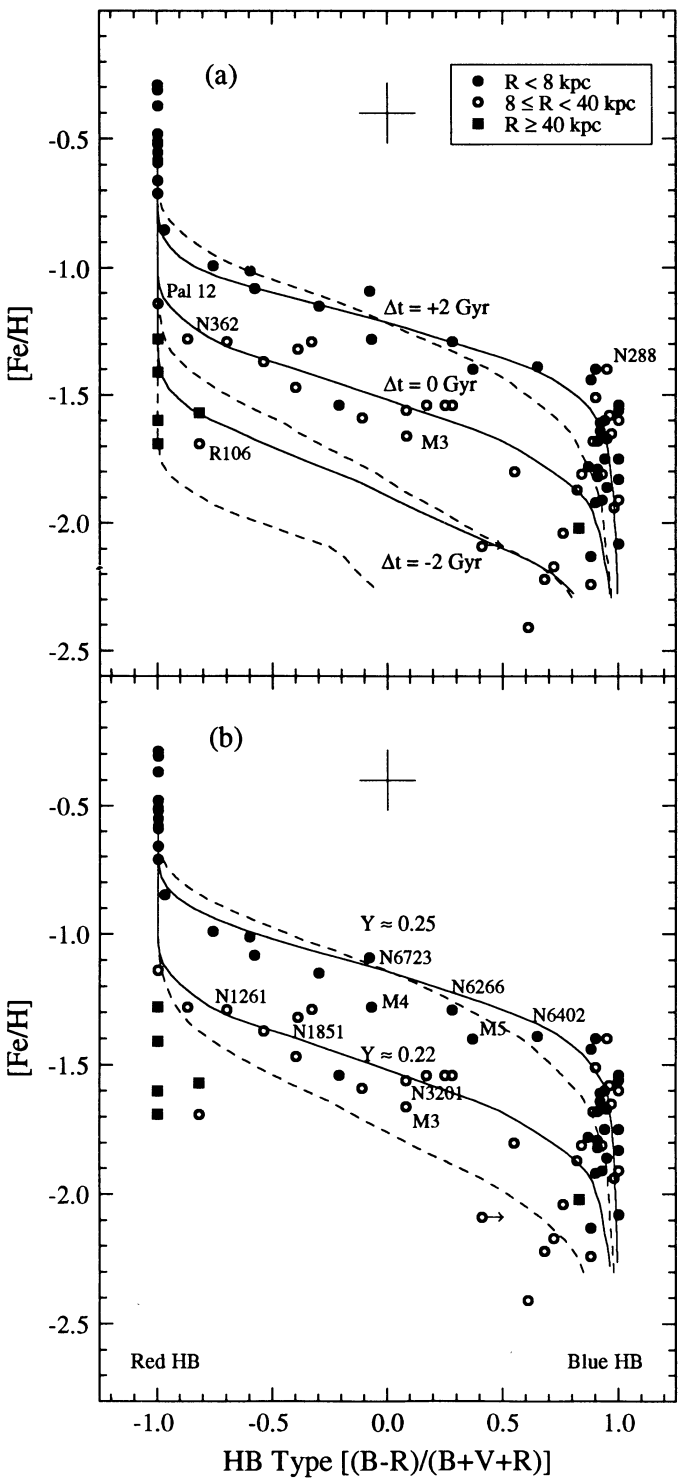


FIG. 9.—(*a*) Same as Fig. 7, but under two different assumptions regarding mass-loss. The dashed lines are for Reimers' (1977) mass-loss relation ($\eta = 0.63$). (*b*) Same as (*a*), but with the assumption that the second parameter is helium abundance.

6.1. *Constraints from Mean Periods and Period Shifts of RR Lyrae Variables*

Figure 9 shows that the differences between the inner halo clusters M4, M5, NGC 6266, and NGC 6723 and the outer halo clusters M3, NGC 3201, NGC 1851, and NGC 1261 may be due to either a difference in age of ~1.5–2 Gyr, or to a difference in He abundance of $Y = 0.02$–0.03, depending on the assumption made regarding mass loss. These alternatives can be tested by examining their effects on the periods of the RR Lyrae variables, which are very sensitive to the luminosity of the HB and hence to Y (see, e.g., Sweigart 1987; Lee & Demarque 1990).

Since the synthetic HB models described in Paper I and § 2 yield the luminosity (L), mass (M), and effective temperature ($T_{\rm eff}$) of each star within the instability strip, it is straightforward to calculate the fundamental periods (P_f) of the model RR Lyrae variables from the period-mean density relation,

$$\log P_f = 0.84 \log L - 0.68 \log M - 3.48 \log T_{\rm eff} + 11.497 , \quad (1)$$

of van Albada & Baker (1971), where P_f is in days and L and M are in solar units. In Figure 10, we compare our model calculations with the values observed (data from Castellani & Quarta 1987) for the differences in the mean fundamentalized periods (mean of type ab's + fundamentalized type c's; $\langle P_f \rangle$) between the clusters of different zones ($R_G < 8$ kpc and $R_G \geq 8$ kpc). The comparison is made for clusters in the ranges $-1.7 < [\mathrm{Fe/H}] < -1.0$ and $-0.7 < (B-R)/(B+V+R) < +0.7$, because only within these ranges do both the inner and the outer halo clusters contain adequate numbers of variables for precise measurements of $\langle P_f \rangle$.

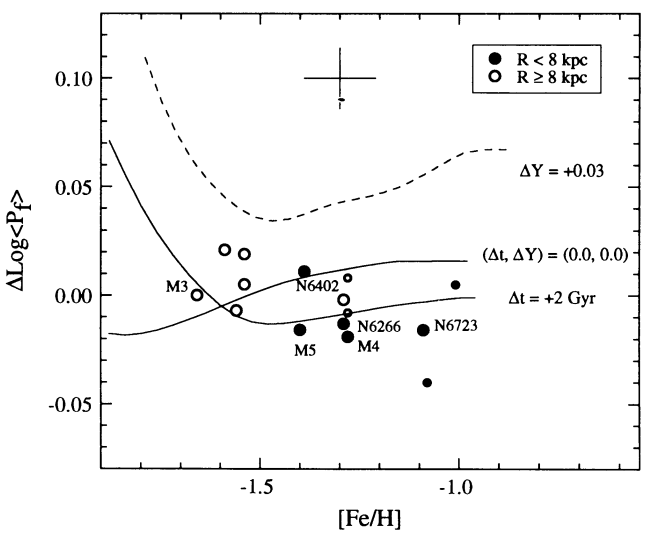


FIG. 10.—The difference in mean fundamentalized period of RR Lyrae stars ($\Delta \log\langle P_f \rangle = \log \langle P_f \rangle_{\rm cluster} - \log \langle P_f \rangle_{\rm M3}$) between the clusters of different radial zones ($R_G < 8$ kpc and $8 \leq R_G < 40$ kpc), assuming the second parameter is either age or helium abundance. If the second parameter is helium abundance, the model calculations for the inner halo ($R_G < 8$ kpc) clusters show that a ΔY of ~0.03 produces a large difference in $\Delta \log \langle P_f \rangle$ that has the opposite sign of the observed difference (*dashed line*). If the second parameter is age, however, the calculations for $\Delta t = 2$ Gyr reproduce, to within the uncertainties, the observed values of $\Delta \log \langle P_f \rangle$ (*solid line*). This is a strong evidence against the helium abundance as the second parameter. See text for similar arguments against the core rotation as the second parameter.

© American Astronomical Society • Provided by the NASA Astrophysics Data System

1994ApJ...423..248L

At one time stellar pulsation calculations suggested that the $T_{\rm eff}$ of both the red and blue edges of the instability strip depended on Y. If this was true, the sensitivity of $\langle P_f \rangle$ to Y would be due to (1) the shift in the locations of these edges and (2) the change in the luminosity of the HB. More recent calculations by Stellingwerf (1984), which include the effects of convection, indicate that there is very little change in the locations of either edge over the range in Y considered here, leaving effect (2) as the only one of significance.

In our calculations, we adopted the results of Tuggle & Iben's (1972) calculations for blue edges of the RR Lyrae instability strip and applied to them the small corrections for convection (see § II*b* of Paper I) suggested by Stellingwerf's (1984) calculations. For the width of the instability strip, we adopted $\Delta \log T_{\rm eff} = 0.065$.

The model calculations presented in Figure 10 show that ΔY of ~ 0.03 produces a large difference in $\Delta \log \langle P_f \rangle$ that has the *opposite* sign of the observed difference. The calculations for $\Delta Y = 0.0$ and an age difference of 1–2 Gyr reproduce, to within the uncertainties, the observed values of $\Delta \log \langle P_f \rangle$ (see also Fig. 9 of Lee 1992b for RR Lyraes in the bulge).

For each variable in M3 and in NGC 6723, which are reddened by only small amounts, the mean value of $T_{\rm eff}$ can be reliably derived from their $(B-V)_0$ colors, which enables a comparison in a plot of log P' against log $T_{\rm eff}$ (see Fig. 11, data described in Paper I). As was the case for $\Delta \log \langle P_f \rangle$, our calculations show that ΔY of ~ 0.03 produces a large shift in log P' ($\Delta \log P' = +0.037$) at constant log $T_{\rm eff}$ between the variables in NGC 6723 and M3 that has the opposite sign of the observed shift [$\Delta \log P' \approx -0.010$, for $\Delta E(B-V) = 0.01$]. The calculations for $\Delta Y = 0.00$ and an age difference of ~ 2 Gyr provide a perfect match ($\Delta \log P' = -0.010$; see Table 1 of Paper I) to the observed shift, which suggests again that there exists little, if any, difference in Y between these clusters.

A similar argument suggests that the second parameter is not the mean rate of core rotation. Since a blue HB is produced by a large mean core rotation, this hypothesis requires that on average there is more rotation in the inner halo clusters than in the outer ones. Our models, which are based on Mengel & Gross (1976) assumptions, indicate that the concomitant differences in the core masses of the RR Lyrae variables are $\Delta M_c \sim 0.043$ (constant mass loss) or $\sim 0.028\ M_\odot$ (variable mass loss). These differences produce significant differences in the luminosity of the HB and consequently period shifts of $\Delta \log P \sim +0.08$ and $+0.05$, respectively. These shifts disagree with the observations in magnitude and in *sign*.

It is important to note that the effects of core rotation calculated by Mengel & Gross (1976), which are the basis of our simulations, depend on a number of simplifications and assumptions. In particular, the assumptions that no angular momentum is removed from the stellar core and that angular momentum is conserved in shells during evolution leads to a substantial overestimate of the angular momentum in the helium core at helium ignition. A more realistic treatment of rotation which includes the removal and redistribution of angular momentum during evolution (Deliyannis, Demarque, & Pinsonneault 1989; Pinsonneault, Kawaler, & De Marque 1990, 1991), shows that the effect of core rotation on the helium core mass is much less than found by Mengel & Gross (1976) and is unlikely to produce sufficiently large variations in core mass to produce the second parameter effect. At any rate, we have seen above that the analysis of period shifts indicates that a variation in core mass whatever its origin, that is large enough to account for the second parameter, produces period shifts that are inconsistent with observations.

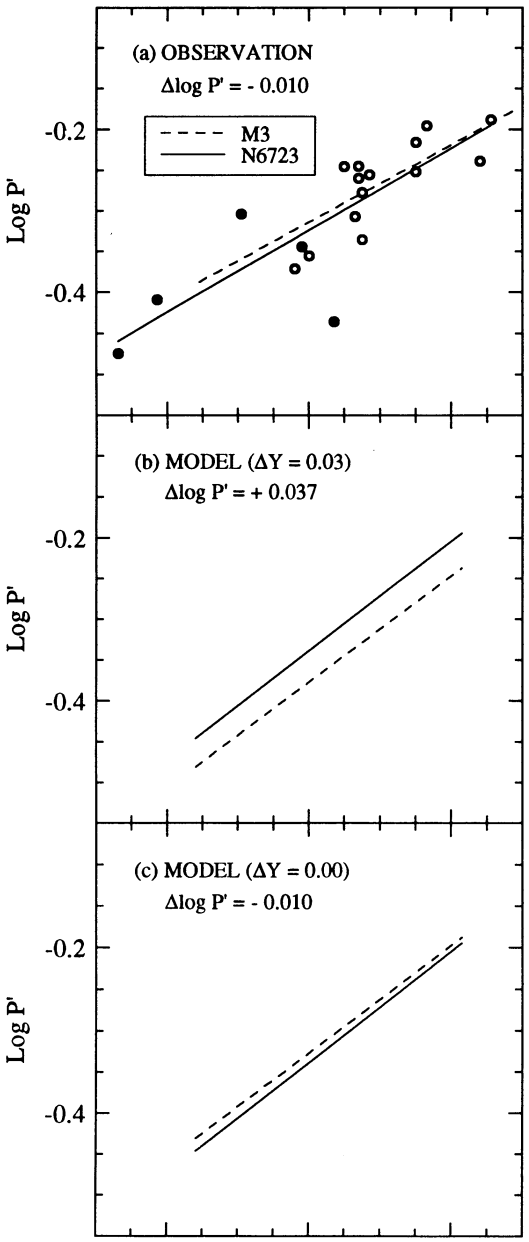


FIG. 11.—Similar to Fig. 10, but for the period shifts at a fixed temperature between the RR Lyraes in M3 and NGC 6723. As was the case for $\Delta \log \langle P_f \rangle$, ΔY of ~ 0.03 produces the period shift (at a fixed $T_{\rm eff}$) that is too large and that has the opposite sign of the observed period shift (panel *b*). If the second parameter is age (and $\Delta Y = 0.00$), however, the model calculations reproduce the observed period shift (panel *c*).

Since the observations of Peterson (1983, 1985a, b) who showed that blue HB stars do rotate, attempts have been made to relate HB rotational velocities to the second parameter. Although there is evidence for some variation in rotation rates from cluster to cluster, the connection with the second parameter is not clear (Pinsonneault et al. 1991). It is important to

© American Astronomical Society • Provided by the NASA Astrophysics Data System

1994ApJ...423..248L

note that the observed HB rotation rates are low and quantitative estimates of the angular momentum lend support to the view that most of the original angular momentum has been transferred out of the HB stars during their earlier evolution (see Fig. 2 of Pinsonneault et al. 1991). The Mengel & Gross (1976) calculations indicate that even the fastest rotation rates observed by Peterson could not account for the core mass dispersion needed for the second parameter (an explanation which is in any case ruled out by the observed period shifts).

Finally, we should mention another explanation of the second parameter due to rotation which has been proposed in the past. In this explanation, it is argued that even though rotation may not affect the HB core mass appreciably, it is capable, through enhanced mass loss, of mimicking the effects of age (Renzini 1977; Fusi Pecci & Renzini 1978; Suntzeff 1981). This then reasonable (but ad hoc) hypothesis has now become difficult to support in view of recent data on cluster photometry near the turnoff which can most naturally be understood in terms of age differences (see below).

The possibility that [CNO/Fe] is the second parameter cannot be tested in a similar way, because the change in HB luminosity that is produced by a difference in [CNO/Fe] is offset by a change in mass at the same HB position and very little change in period results (see, Sweigart et al. 1987; Dorman et al. 1991; Lee 1991b). We will discuss below, however, that both direct spectroscopic observations and the recent calculations of turnoffs and HB's with CNO enhancements provide strong evidence against the hypothesis that [CNO/Fe] is the second parameter.

6.2. *Constraints from Main-Sequence Turnoffs*

The famous pair of clusters NGC 288 and 362 provide a well-documented case where [CNO/Fe] cannot be the global second parameter. These clusters, which have nearly the same [Fe/H], differ markedly in HB type (+0.95 and −0.87, respectively, for 288 and 362) and noticeably in the luminosity of the main-sequence turnoff, in the sense that the turnoff of NGC 288 is ~0.2 mag fainter than that of 362 (see Bolte 1989; Green & Norris 1990). As discussed by Demarque et al. (1988), the relatively bright turnoff of NGC 362 is incompatible with the hypothesis that the redness of its HB is solely due to larger [CNO/Fe] than NGC 288. An enhancement in CNO shortens the M-S lifetimes of the stars (see VandenBerg 1985). Hence if NGC 362 is the same age as NGC 288 but CNO enhanced, it should have a fainter rather than a brighter turnoff than NGC 288. Furthermore, the spectroscopic observations of red giants in these clusters by Dickens et al. (1991) rule out a difference in CNO as large as that required to explain the difference in HB morphology. We show below that the differences in both M-S luminosity and HB type are consistent with an age difference of ~3 Gyr.

Additional evidence against the hypothesis that [CNO/Fe] is the second parameter is presented in Figure 12, where for inner and outer halo clusters the V mag difference between the turnoff and the HB, ΔV(TO − HB), is plotted against [Fe/H] (values of ΔV from Buonanno, Corsi, & Fusi Pecci 1989 and Chaboyer, Sarajedini, & Demarque 1992). Two clusters of the *same* [Fe/H] and age, but different [CNO/Fe], will have different values of ΔV(TO − HB) because of two competing effects. The cluster with enhanced [CNO/Fe] will have, as noted above, a fainter turnoff. It will also have, however, a slightly fainter HB within the instability strip (see Dorman et al. 1991).

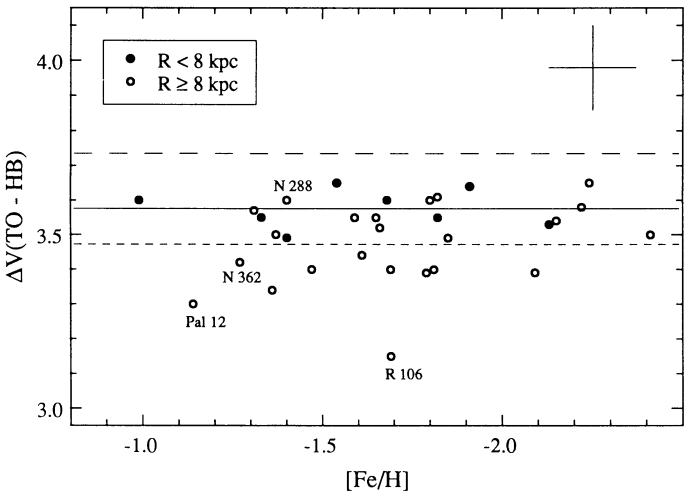


FIG. 12.—The values of ΔV(TO − HB) derived from the recent CCD photometry (mostly from Buonanno et al. 1989) are plotted against [Fe/H] for globular clusters in two radial zones of the Galaxy (see text).

The first effect overwhelms the second, and consequently, the enhanced [CNO/Fe] cluster has a larger value of ΔV(TO − HB). In Figure 12, the solid line is drawn at the mean value of ΔV (TO − HB) of the inner halo clusters (the closed circles). The long-dashed line is drawn at the value of ΔV(TO − HB) expected to be the mean of the outer halo clusters (open circles), if they are enhanced by 0.5 dex in [CNO/Fe] with respect to the inner halo clusters (estimated from the calculations of VandenBerg 1985). This amount of enhancement is required to explain the mean difference in HB type between the inner and outer halos (Table 2). There is no evidence from Figure 12 that the outer halo clusters have larger values of ΔV(TO − HB) than the inner halo clusters. In fact, in direct contradiction to this hypothesis, the outer halo clusters have a *smaller* mean ΔV(TO − HB) than the inner halo clusters (see short-dashed line). This difference, ~0.11 mag. (ignoring R106), is consistent with ~1.5 Gyr difference in mean age, as predicted by the age hypothesis for the second parameter (see Table 2).

7. TESTING THE AGE HYPOTHESIS

The above analysis casts doubts on every candidate second parameter except cluster age. A comparison of the ages derived from M-S turnoffs and those inferred from HB morphology provides a direct test of the age hypothesis. For both methods, the uncertainties in the age difference are minimized if the comparison is between clusters of nearly the same [Fe/H]. Below we consider three such pairs of clusters, for which the predicted age differences are larger and for which there exists particularly good data.

7.1. *NGC 288 and NGC 362*

In Figure 13, the observed HB's of this pair of clusters (data from Harris 1982 and Buonanno et al. 1984) are compared with our synthetic models, which include the scatter expected from the random errors in magnitude and in color as estimated by the observers. On the basis of the values of [Fe/H] given by Zinn & West (1984) and Armandroff & Zinn (1988) for these clusters ([Fe/H] = −1.40 and −1.28, for 288 and 362, respectively), we adopted $Z = 0.0007$ and $Z = 0.001$ in our

© American Astronomical Society • Provided by the NASA Astrophysics Data System

1994ApJ...423..248L

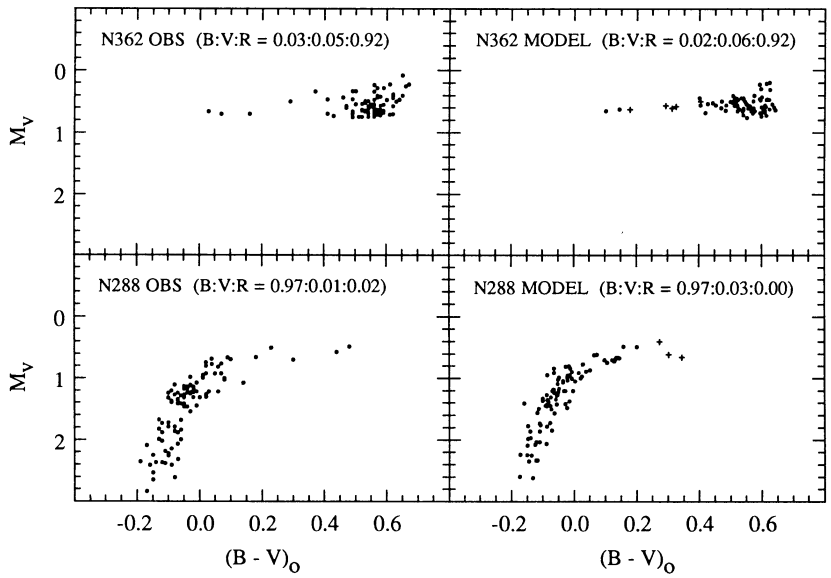


FIG. 13.—Comparison of observations and synthetic HBs for NGC 288 and NGC 362. No RR Lyrae variables are plotted in the observational diagrams.

model calculations. We also used the same dispersion in mass ($\sigma_M = 0.025\ M_\odot$), He abundance ($Y_{HB} = 0.244$), and O abundance ([O/Fe] = 0.0) for each cluster. One can see from Figure 13 that our synthetic HB models reproduce the major features of the HB's of the two clusters. Our model for NGC 288, which is based on our standard assumption of truncated Gaussian dispersion in M_{HB} (see § II*b* of Paper I), even has a gap at approximately the same location as the observed one. Although the statistical evidence for the presence of this gap is not strong (see § 7.2 below), its presence in the synthetic HB models is of significance because it can be understood in terms of the morphology of HB evolutionary tracks (see also Lee et al. 1988a for a discussion of models that reproduce the uneven color distribution in some other clusters).

The following procedure is used to estimate the difference in age from HB morphology once a good match is obtained between the observed and model HB's. The HB models yield the mean masses of the HB stars in the clusters, $\langle M_{HB}\rangle$ ($=0.644 \pm 0.015$ and $0.738 \pm 0.015\ M_\odot$ for 288 and 362, respectively). Since the mean amount of mass-loss suffered by red giants cannot be estimated accurately from theory, it is necessary to adopt a value for the age of one of the two clusters from the luminosity of its M-S turnoff. The isochrone for the appropriate composition that matches this luminosity provides the mass (M_{RG}) of a red giant at the tip of the giant branch in the absence of mass loss. The difference between M_{RG} and $\langle M_{HB}\rangle$ is then the mean amount of mass loss that occurred in the first cluster. To obtain M_{RG} for the second cluster, this value is then either simply added to $\langle M_{HB}\rangle$ (constant mass-loss assumption) or first corrected for the effects considered by Reimers (variable mass-loss assumption). To estimate the age of the second cluster, its value of M_{RG} is compared with the values given by isochrones spanning a range in ages. The difference between the resulting age and the one adopted for the first cluster is the age difference, Δt_{HB}, predicted from HB morphology.

In an earlier report (Lee et al. 1988b), we obtained $\Delta t_{HB} =$ 5–6 Gyr for NGC 288 and 362, in the sense that NGC 288 is older. This was based in part on the age of 18.5 Gyr that we adopted from the M-S turnoff of NGC 288. At the time, this value of Δt_{HB} was in reasonable agreement with the ages derived from the M-S turnoffs, which, however, were based on heterogeneous data sets. Since then, the observational situation has improved significantly due to the precise differential photometry reported by Bolte (1989) and by Green & Norris (1990). These authors found that an age difference of ~ 3 Gyr provides an excellent explanation of the observed morphological differences in the vicinity of the turnoffs. VandenBerg et al. (1990) and independently Sarajedini & Demarque (1990) have recently confirmed this using a new method based on the difference in color between the turnoff and the base of the giant branch, which can potentially detect variations of less than < 1 Gyr in age. Because the age difference, ~ 3 (± 1.5) Gyr, found in these investigations is significantly smaller than our earlier estimate of ≥ 5 Gyr, it is reasonable to question if age can be the sole second parameter, as have VandenBerg et al. (1990). This possibility has motivated us to examine critically the steps involved in the transformation of the difference in $\langle M_{HB}\rangle$ into an age difference.

As noted by Lee (1991a), this transformation depends sensitively on the age adopted in the step where an isochrone is used to estimate M_{RG} for the first cluster, because the relationship between M_{RG} and age is nonlinear (see Fig. 6 of Lee 1991b). In Figure 14, the age difference between NGC 288 and NGC 362, Δt_{HB}(N288-N362), is plotted against the age of NGC 288. One can see that Lee et al. (1988b) obtained Δt_{HB}(N288-N362) ≥ 5 Gyr because they adopted a large age (18.5 Gyr) for NGC 288. If instead, the age of NGC 288 is ~ 14 Gyr, Δt_{HB}(N288-N362) is reduced to 3–4 Gyr. (The amount of mass loss, $\Delta M = M_{RG} - \langle M_{HB}\rangle$, required to match the observed HB morphology then increases from ~ 0.15 to $\sim 0.22\ M_\odot$).

Our earlier estimate for 18.5 Gyr for the age of NGC 288 is probably an overestimate for the following two reasons: First, the value that was adopted for the V mag of its M-S turnoff (19.1) is probably too faint. This value was given by the mean of several photographic observations and the CCD photometry by Pound, James, & Heasley (1987). The most recent CCD data (Bolte 1991, private communication; see also Van-

© American Astronomical Society • Provided by the NASA Astrophysics Data System

1994ApJ...423..248L

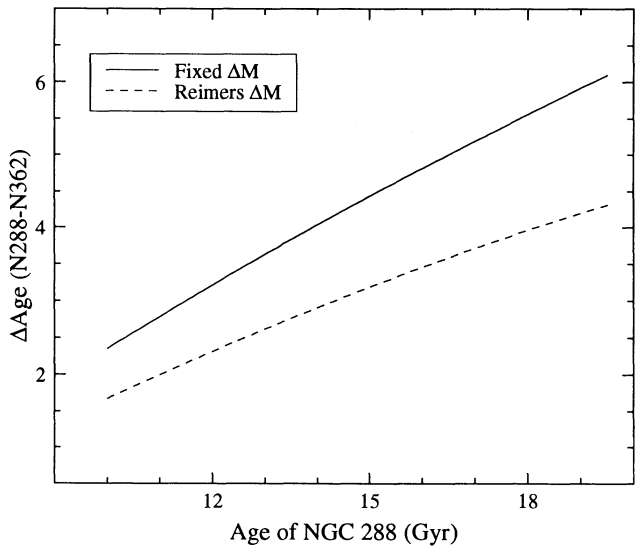


FIG. 14.—The age difference between NGC 288 and 362 estimated from HB morphology as a function of the absolute age for NGC 288 (see text).

denBerg et al. 1990) suggests that this value is probably too faint by 0.1–0.2 mag, in which case it caused an overestimate of 1.5–3 Gyr in age. Second, we assumed [O/Fe] = 0.0 for NGC 288 and 362, whereas the recent spectroscopic observations by Dickens et al. (1991) indicate [O/Fe] $\approx$ 0.2 for both clusters. By itself, this incorrect assumption led to an overestimate of $\sim$1.1 Gyr for the age of NGC 288.

To derive a best estimate of Δt_{HB}(288–362), we have adopted 14.9 Gyr for the age of NGC 288 (Chaboyer et al. 1992). Following Chieffi, Straniero, & Salaris (1991), we have made small corrections to the values of $\langle M_{HB} \rangle$ given by our synthetic HB calculations so that they also correspond to [α/Fe] = 0.2. For Δt_{HB}(288–362), we obtain 3–4 Gyr, which is in good agreement with the age differences obtained from either the M-S turnoff luminosities (Bolte 1989; Green & Norris 1990) or the color differences between the turnoff and the base of the giant branch (VandenBerg et al. 1990; Sarajedini & Demarque 1990).

7.2. *Ruprecht 106 and NGC 6752*

The *C-M* diagram constructed by Buonanno et al. (1990) for R106 revealed that it is a metal-poor cluster ([Fe/H] = -1.9) with a red HB [$(B-R)/(B+V+R) = -0.82$] and a relatively bright M-S turnoff. From the luminosity of the turnoff, Buonanno et al. estimated that R106 is $\sim$4–5 Gyr younger than the metal-poor and blue HB clusters NGC 6397 and M68, which they suggested is consistent with the age hypothesis for the second parameter. More recently, Da Costa et al. (1992) observed the infrared Ca II lines in the spectra of several red giants in R106 and in several other clusters, including NGC 6752. Their observations yielded a slightly higher [Fe/H] for R106 (-1.69 ± 0.05) than Buonanno et al. had inferred from the color of the giant branch, $(B-V)_{0,g}$. Da Costa et al. made a detailed comparison of the M-S turnoffs of R106 and NGC 6752, which is more metal rich ([Fe/H] = -154 ± 0.09; Zinn & West 1984), but has a much bluer HB [$(B-R)/(B+V+R) = 1.00$]. From the difference in color between the turnoff and the base of the giant branch and by the ΔV(TO – HB) method, Da Costa et al. deduced that R106 is 3 ± 2 Gyr younger than NGC 6752. They concluded that this is additional evidence that age is contributing to the second parameter phenomenon, but they also noted that detailed modeling of the HB's was required before one could conclude if age is the sole second parameter.

In Figure 15, our models for the HB's of R106 and NGC 6752 are compared with the observations of these clusters by Buonanno et al. (1986b, 1990). There is a good match between our model and the observations for R106. Because the HB of NGC 6752 is unusually long and appears to have gaps at $M_v \sim +2.0$ and $+3.4$, it is very challenging to model. Our first model (A), which was constructed under our standard assumptions ($\sigma_M = 0.03\ M_\odot$), has a gap at approximately the same location as one of the two gaps in NGC 6752. This gap and the one noted earlier in our model for NGC 288 are caused by the change in the morphology of the post-ZAHB tracks at approximately this luminosity. Many runs of our synthetic HB code with the same input parameters indicate that the prominence of this gap is very variable, for it depends on the precise distribution of the star along the post-ZAHB tracks. This suggests that the details of HB morphology, including the magnitude of the gaps, are subject to stochastic effects which differ from cluster to cluster. Hence, the absence of this gap in the HB's of some clusters may not mean that they are different from NGC 6752 in some fundamental way.

Model A obviously fails to reproduce the long blue tail of NGC 6752. Consequently, we have constructed another model (B) using a larger value for the dispersion in mass ($\sigma_M = 0.05\ M_\odot$). A better match to the length of the HB in 6752 is obtained, but at the expense of making σ_M a variable parameter. We could have also obtained a reasonable match by replacing the truncated Gaussian for the mass distribution in our models with some other function specifically designed for NGC 6752. The resort to either technique underscores the need for some additional parameter to explain the long HB in NGC 6752 and in a few other clusters.

This uncertainty has some impact on the age difference that one infers for R106 and NGC 6752 from their HB morphologies. If the unknown parameter primarily affects the wings of the distribution in mass on the HB, as appears to be the case, it will have only a minor effect on the inferred age difference, which is estimated from the difference in $\langle M_{HB} \rangle$. For example, our model B yields a $\sim$1 Gyr older age for NGC 6752 than model A. A smaller difference would have been obtained if we had not assumed in model B a symmetric distribution in M_{HB} about $\langle M_{HB} \rangle$, but instead one skewed toward low masses in order to fit the blue tail of NGC 6752.

For the difference in age between R106 and NGC 6752 our model B yields 4.9–7.4 Gyr, depending on whether variable or constant mass-loss is assumed. This is somewhat larger than the value, 3 ± 2 Gyr, that Da Costa et al. (1992) estimated.[1] If [α/Fe] = $+0.4$ is assumed instead of 0.0 for both clusters, our estimates are reduced by $\sim$0.8 Gyr. If the value of $\langle M_{HB} \rangle$ given by model A is more nearly correct, the age difference is reduced by $\sim$1 Gyr. Finally, if NGC 6752 is younger than 15 Gyr, our assumed age, the age difference will drop again. While the uncertainties are many, we conclude that the difference in age between R106 and NGC 6752 that is inferred from their M-S turnoffs can account for at least most of the difference in $\langle M_{HB} \rangle$ between the two clusters. Obviously, some additional variable is required to explain the blue tail of NGC 6752.

[1] But, note that Chaboyer et al. (1992) get an age difference of $\sim$6 Gyr on the basis of α-enhanced tracks using the ΔV(TO – HB) method.

© American Astronomical Society • Provided by the NASA Astrophysics Data System

1994ApJ...423..248L

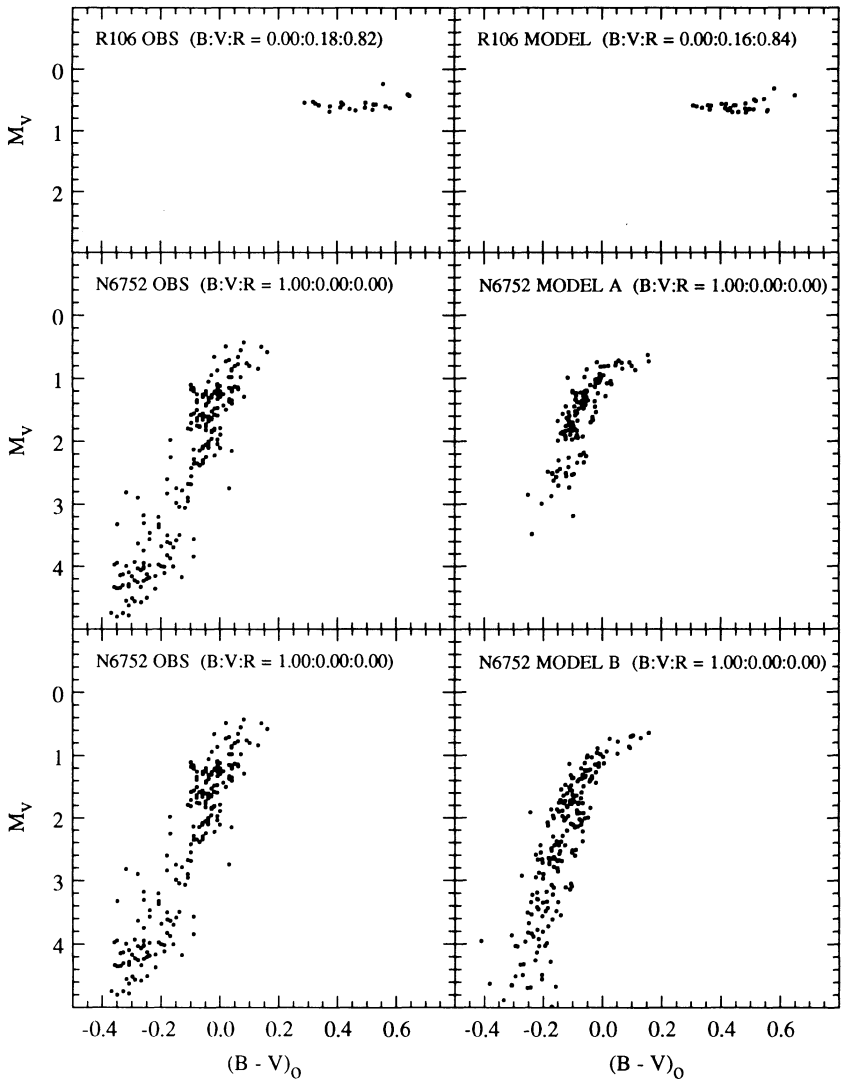


FIG. 15.—Same as Fig. 13, but for Ruprecht 106 and NGC 6752. For NGC 6752, two alternative models are presented.

7.3. *Ruprecht 106 and NGC 6397*

After completing the above analysis, we learned of the new photometric investigation of R106 by Buonanno et al. (1993), in which they present additional evidence that it is both very metal poor and relatively young. From the position and slope of the giant branch in the M_I, $(V-I)_0$, *C-M* diagram, they obtained $[\mathrm{Fe/H}] = -1.9 \pm 0.2$ for R106. While this measurement is consistent to within the errors with the spectroscopic observations of Da Costa et al. (1992), it suggests that NGC 6752 may not be the optimum cluster to compare with R106. A better object may be NGC 6397, which has $[\mathrm{Fe/H}] = -1.9 \pm 0.14$ and a very blue HB $[(B-R)/(B+V+R) = 0.93]$.

In the left-hand panel of Figure 16, we have plotted the HB stars (data from Buonanno et al. 1990 and Alcaino et al. 1987) and the M-S and giant branch ridge lines of R106 and NGC 6397. The fiducial sequence shown for R106 is taken from Buonanno et al. (1993), while that for NGC 6397 was derived from the data provided by Stetson (1991, private communication; see VandenBerg et al. 1990). In the right-hand panel, we show the synthetic HB models which reproduce the observed HBs. As noted earlier, NGC 6397 is a very highly concentrated cluster with a very large central density, much like NGC 6752. The HB of NGC 6397 has none of the peculiarities of NGC 6752's, and our standard assumption for the mass dispersion yields an excellent match. Solar abundance ratios were assumed in our calculations; hence our results are at odds with the conclusion of Buonanno et al. (1993) that the redness of the HB in R106 is necessarily indicative of an α element enhancement. Our results for the difference in age between R106 and NGC 6397 would change by an insignificant amount if we adopted equal α enhancements for both clusters. A large difference between R106 and NGC 6397 in the α/Fe ratio seems unlikely given their HB morphologies and M-S turnoffs (see Buonanno et al. 1993). Adopting an age of 15 Gyr for NGC 6397, we find from our HB models that R106 is younger by either 3.6 Gyr (variable mass loss) or 5.4 Gyr (const. mass loss). In the right-hand panel of Figure 16, we have plotted the Revised Yale Isochrones for $Z = 0.00023$, $Y = 0.23$, and an age difference of 4.5 Gyr. The similarity between these isochrones

© American Astronomical Society • Provided by the NASA Astrophysics Data System

1994ApJ...423..248L

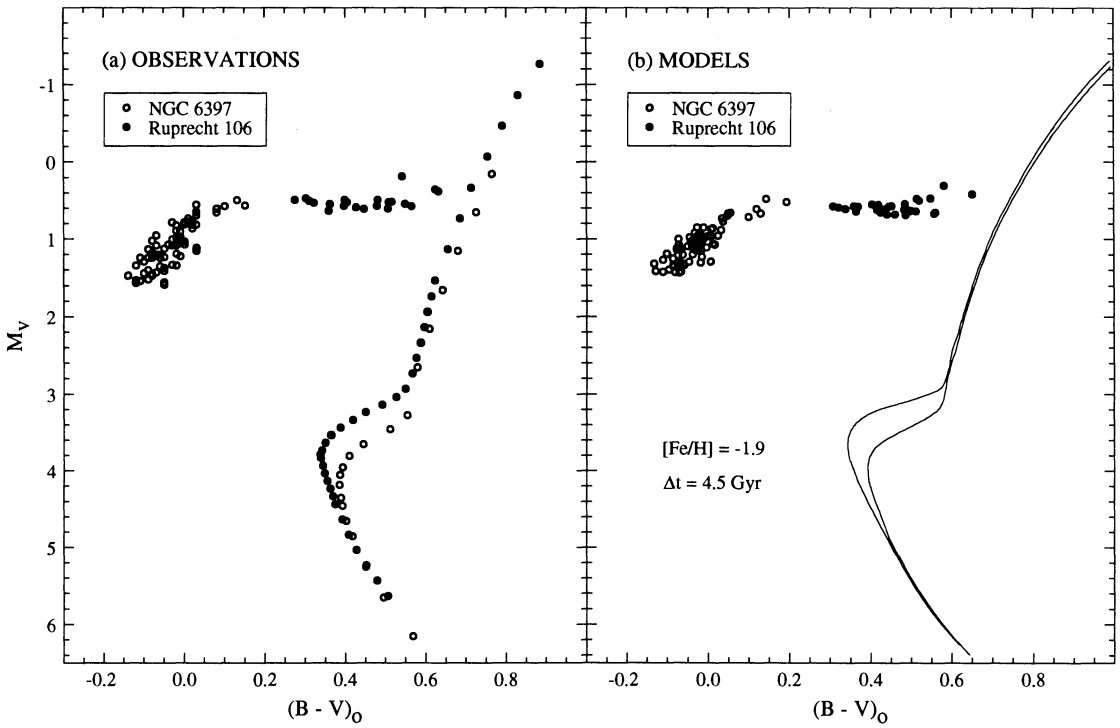


FIG. 16.—(*a–b*) The observational C-M diagrams (individual HB stars + MS and giant-branch fiducial sequences) for Ruprecht 106 and NGC 6397 are compared with the models (synthetic HB's + Revised Yale Isochrones), assuming that NGC 6397 is older by ~4.5 Gyr. The observational diagrams are transformed to the absolute scales using the Lee (1992c) RR Lyrae distance scale ($V - M_v = 17.27$ and 12.35 for R106 and NGC 6397, respectively), and assuming $E(B-V) = 0.23$ and 0.18 for R106 and NGC 6397, respectively.

and the ridge lines plotted in the left-hand panel suggests that an age difference of about this size is also indicated by the M-S turnoffs. In fact, from a detailed analysis of the turnoffs, Buonanno et al. (1993) concluded that R106 is 4–5 Gyr younger than typical metal-poor clusters such as NGC 6397. Thus, in the case of R106 and NGC 6397, there is good agreement between the age difference inferred from HB morphology and the M-S turnoff.

In summary, for each pair of clusters considered here there is substantial evidence for real differences in age. In the cases of NGC 288 and 362, and R106 and NGC 6397, the agreement between the age differences inferred from HB morphology and from the M-S turnoff are within the errors, and there is little need for additional hypotheses to explain the differences in HB morphology. This is less clear in the case of R106 and NGC 6752, because the origin of the long blue tail in NGC 6752 is unknown and because the O/Fe ratios of the clusters have not been measured.

8. DISCUSSION

Our major results are that the variation in HB morphology with R_G cannot be explained by variations in He, CNO/Fe, core rotation (M_c), or the new candidate second parameters: concentration, central density and luminosity, and that age variations of the magnitude necessary to explain the effect are compatible with the existing observational data. The "loose ends" remain the origin of the blue tails and gaps in the HB's of some clusters and the O/Fe ratios of the clusters, which have a profound effect on the values of the age differences that one infers from both HB morphology and the M-S turnoff. Although the importance of the O/Fe ratio to the determination of cluster ages cannot be overstated, for the reasons given in §§ 6 and 7, it must play a secondary role to age as a second parameter.

The major implications are that the inner halo globular clusters and field stars are older in the mean and have more uniform ages than the clusters and stars in the outer halo (see SZ; Zinn 1980; Lee et al. 1988b; Lee 1991a, 1992a, b).[2] Similar gradients with greater ages among field halo stars toward the Galactic center have also been observed by Preston, Shectman, & Beers (1991) and Suntzeff, Kinman, & Kraft (1991). The recent investigation by Lee (1992b) of the RR Lyrae variables in Baade's window suggests that the same trend extends even to the central bulge of the Galaxy, for its most metal poor population appears to be even older than the stars and clusters of the inner halo. One has then a picture of formation where the innermost region of the proto-Galaxy formed first and was the core around which the remainder continued to accumulate over several gigayears (i.e., the SZ scenario; see § 4 of Lee 1992b). The observational and theoretical support for this chronology is now sufficiently well advanced that it is a strong discriminant against alternative pictures of formation.

[2] We emphasize that we do not imply that there is a tight age–R_G relationship in the Galaxy, only that the inner halo is more homogeneous in age than the outer halo. We predict that both young and old clusters coexist in the outer halo. Indeed, some very old clusters are observed at large R_G (see VandenBerg et al. 1990 and Fig. 4 of Chaboyer et al. 1992).

© American Astronomical Society • Provided by the NASA Astrophysics Data System

1994ApJ...423..248L

We thank an anonymous referee for so carefully reading an early draft of this paper and for making some useful comments. Y.-W. L. was supported by NASA through a grant HF-1014.01-90A and by Yonsei University through a grant 93-120. R. Z. and P. D. acknowledge the support of NSF (AST 89-14519) and NASA (NAG 5-1486, NAGW-2469) grants, respectively.

REFERENCES

Aaronson, M., Schommer, R. A., & Olszewski, E. W. 1984, ApJ, 276, 221
Alcaino, G. 1972, A&A, 16, 220
———. 1977, A&AS, 29, 9
———. 1979a, A&AS, 35, 233
———. 1979b, A&AS, 38, 61
———. 1980, A&AS, 39, 315
———. 1981, A&AS, 44, 191
———. 1983, A&AS, 52, 105
Alcaino, G., Buonanno, R., Caloi, V., Castellani, V, Corsi, C. E., Iannocola, G., & Liller, W. 1987, AJ, 94, 917
Alcaino, G., & Liller, W. 1980, AJ, 85, 1330
———. 1983, AJ, 88, 1166
———. 1986, A&A, 161, 61
Armandroff, T. E.1988, AJ, 96, 588
———. 1989, AJ, 97, 375
Armandroff, T. E., & Da Costa, G. 1991, AJ, 101, 1329
Armandroff, T. E., Da Costa, G. S., & Zinn, R. 1992, AJ, 104, 164
Armandroff, T. E., & Zinn, R. 1988, AJ, 96, 92
Bailyn, C. D., Sarajedini, A., Cohn, H., Lugger, P. M., & Grindlay, J. E. 1992, AJ, 103, 1564
Barbon, R. 1965, Asiago, Contr., No. 175
Bolte, M. 1989, AJ, 97, 1688
Buonanno, R. 1993, in The Globular Cluster-Galaxy Connection, ed. G. Smith & J. Brodie (San Francisco: ASP), in press
Buonanno, R., Buscema, G., Fusi Pecci, F., Richer, H. B., & Fahlman, G. G. 1990, AJ, 100, 1811
Buonanno, R., Buzzoni, A., Corsi, C. E., Fusi Pecci, F., & Sandage, A. 1986a, Mem. Soc. Astron. Ital., 57, 391
Buonanno, R., Caloi, V., Castellani, V., Corsi, C., Fusi Pecci, F., & Gratton, R. 1986b, A&AS, 66, 79
Buonanno, R., Corsi, C. E., Ferraro, I., & Fusi Pecci, F. 1987, A&AS, 67, 327
Buonanno, R., Corsi, C. E. & Fusi Pecci, F. 1985, A&A, 145, 97
———. 1989, A&A, 216, 80
Buonanno, R., Corsi, C. E., Fusi Pecci, F., Alcaino, G., & Liller, W. 1984, ApJ, 277, 220
Buonanno, R., Corsi, C. E., Fusi Pecci, F., Richer, H. B., & Fahlman, G. G. 1993, AJ, 105, 184
Buonanno, R., Fusi Pecci, F., Cappellaro, E., Ortolani, S., Richtler, T., & Geyer, E. H. 1991, AJ, 102, 1005
Byun, Y.-I., & Lee, Y.-W. 1991, in Proc. ASP Symp. on The Formation and Evolution of Star Clusters, ed. K. Janes (San Francisco: ASP), 243
Caloi, V., Castellani, V., & Piccolo, F. 1987, A&AS, 67, 181
Cannon, R. D. 1981, in IAU Colloq. 168, Astrophysical Parameters for Globular Clusters, ed. A. G. D. Philip & D. S. Hayes (Schenectady: L. Davis), 501
Cannon, R. D., Sagar, R., & Hawkins, M. R. S. 1990, MNRAS, 243, 151
Carney, B. W., Fullton, L., & Trammell, S. P. 1991, AJ, 101, 1699
Carney, B. W., Latham, W., & Laird, J. B. 1990, AJ, 99, 572
Castellani, V. 1983, Mem. Soc. Astron. Ital., 54, 141
Castellani, V., & Quarta, M. L. 1987, A&AS, 71, 1
Chaboyer, B., Sarajedini, A., & Demarque, P. 1992, ApJ, 394, 515
Chieffi, A., Straniero, O., & Salaris, M. 1991, in Proc. ASP Sympsium on The Formation and Evolution of Star Clusters, ed. K. Janes (San Francisco: ASP), 219
Christian, C. A. & Heasley, J. N. 1986, ApJ, 303, 216
Cudworth, K. M. 1985, AJ, 90, 65
———. 1986, AJ, 92, 348
Cuffey, J. 1965, AJ, 70, 732
Da Costa, G. S. 1985, ApJ, 291, 230
Da Costa, G. S., Armandroff, T. E., & Norris, J. E. 1992, AJ, 104, 154
Da Costa, G. S., & Seitzer, P. 1985, AJ, 97, 405
Deliyannis, C. P., Demarque, P., & Pinsonneault, M. H. 1989, ApJ, 347, L73
Demarque, P. 1980, in IAU Symp. 85, Star Clusters, ed. J. E. Hesser (Dordrecht: Reidel), 281
Demarque, P., Lee, Y.-W., Zinn, R., & Green, E. M. 1988, in The Abundance Spread within Globular Clusters: Spectroscopy of Individual Stars, ed. G. Cayrel de Strobel, M. Spite, & T. L. Evans (Paris: Paris Obs.), 97
Dickens, R. J. 1972, MNRAS, 157, 281
Dickens, R. J., Croke, B. F. W., Cannon, R. D., & Bell, R. A. 1991, Nature, 351, 212
Dickens, R. J., & Rolland, A. 1972, MNRAS, 160, 37
Djorgovski, S. G., & Piotto, G. 1992, AJ, 104, 2112
Dorman, B., Lee, Y.-W., & VandenBerg, D. A. 1991, ApJ, 366, 115
Faulkner, J. 1966, ApJ, 144, 978
Fusi Pecci, F., Ferraro, F., Bellazzini, M., Djorgovski, S., Piotto, G., & Buonanno, R. 1992, AJ, 105, 1145.
Fusi Pecci, F., & Renzini, A. 1978, in The HR Diagram, ed. A. G. D. Philip & D. S. Hayes (Dordrecht: Reidel), 225
Gratton, R. G., & Ortolani, S. 1984, A&AS, 57, 177
Gratton, R. G., & Ortolani, S. 1988, A&AS, 73, 137
Green, E. M., Demarque, P., & King, C. R. 1987, The Revised Yale Isochrones and Luminosity Functions, (New Haven: Yale Univ. Obs.)
Green, E. M., & Norris, J. 1990, ApJ, 353, L17
Harris, W. E. 1975, ApJS, 29, 397
———. 1982, ApJS, 50, 573
———. 1990, in The Bulges of Galaxies, ed. B. J. Jarvis & D. M. Terndrup (Garching: ESO), 153
Harris, W. E., & Racine, R. 1973, AJ, 78, 242
———. 1974, AJ, 79, 472
Harris, W. E., Racine, R., & de Roux, J. 1976, ApJS, 31, 13
Harris, W. E., & van den Bergh, S. 1984, AJ, 89, 1816
Hartwick, F. D. A. 1975, PASP, 87, 77
Hartwick, F. D. A., & Hesser, J. E. 1972, ApJ, 175, 77
———. 1973, ApJ, 186, 1171
Hartwick, F. D. A., & Sandage, A. 1968, ApJ, 153, 715
Hesser, J. E., Harris, W. E., VandenBerg, D. A., Allwright, J. W. B., Shott, P., & Stetson, P. B. 1987, PASP, 99, 739
Hogg, H. S. 1973, Pub. David Dunlap Obs., Vol. 3, No. 6
Janes, K. A., & Heasley, J. N. 1991, AJ, 101, 2097
Kogan, C. S., Wehlau, A., & Demers, S. 1974, AJ, 79, 387
Lee, S.-W. 1977a, A&AS, 27, 367
———. 1977b, A&AS, 28, 409
———. 1977c, A&AS, 29, 1
Lee, Y.-W. 1989, Ph.D. thesis, Yale University
———. 1990, ApJ, 363, 159
———. 1991a, in Proc. ASP Symp. on The Formation and Evolution of Star Clusters, ed. K. Janes (San Francisco: ASP), 205
———. 1991b, ApJ, 373, L43
———. 1992a, PASP, 104, 798
———. 1992b, AJ, 104, 1780
———. 1992c, Mem. Soc. Astr. Ital., 63, 331
Lee, Y.-W., & Demarque, P. 1990, ApJS, 73, 709
Lee, Y.-W., Demarque, P., & Zinn, R. 1988a, in IAU Symp. 126, Globular Cluster Systems in Galaxies, ed. J. E. Grindlay & A. G. D. Philip (Dordrecht: Kluwer), 505
———. 1988b, in Calibration of Stellar Ages, ed. A. G. D. Philip (Schenectady: L. Davis), 141
———. 1990, ApJ, 350, 155 (Paper I)
Light, R. 1988, PhD thesis, Yale University
Liller, M. H. 1980a, AJ, 85, 673
———. 1980b, AJ, 85, 1480
Liller, M. H., & Carney, B. 1978, ApJ, 224, 383
Lin, D. N., & Richer, H. B. 1992, ApJ, 388, L57
Mengel, J. G., & Gross, P. G. 1976, A&SS, 41, 407
Menzies, J. 1972, MNRAS, 156, 207
———. 1974, MNRAS, 168, 177
Norris, J. E., & Ryan, S. G. 1991, ApJ, 380, 403
Ortolani, S., & Gratton, R. G. 1990, A&A, 82, 91
Peterson, R. C. 1983, ApJ, 275, 737
———. 1985a, ApJ, 289, 320
———. 1985b, ApJ, 294, L35
Philip, A. G. D., Cullen, M. F., & White, R. E. 1976, Dudley Obs. Rept., No. 11
Pike, C. D. 1976, MNRAS, 177, 257
Pinsonneault, M. H., Deliyannis, C. P., & Demarque, P. 1991, ApJ, 367, 239
Pinsonneault, M. H., Kawaler, S. D., & Demarque, P. 1990, ApJS, 74, 501
Pound, M. W., Janes, K. A., & Heasley, J. N. 1987, AJ, 94, 1185
Preston, G. W., Schectman, S. A., & Beers, T. C. 1991, ApJ, 375, 121
Racine, R. 1971, AJ, 76, 331
Racine, R., & Harris, W. E. 1975, ApJ, 196, 413
Reimers, D. 1977, A&A, 57, 395
Renzini, A. 1977, in Advanced Stages in Stellar Evolution, ed. P. Bouvier & A. Maeder (Geneva: Geneva Obs.), 149
Renzini, A. 1983, Mem. Soc. Astro. Ital., 54, 335
Richer, H. B., & Fahlman, G. G. 1987, ApJ, 316, 189
Rood, R. T. 1973, ApJ, 184, 915
———. 1981, in Physical Processes in Red Giants, ed. I. Iben, Jr., & A. Renzini (Dordrecht: Reidel), 51
Rood, R. T., & Seitzer, P. O. 1981, in IAU Colloquium No. 68, Astrophysical Parameters for Globular Clusters, ed. A. G. D. Philip & D. S. Hayes (Schenectady: L. Davis), 369
Sandage, A. 1966, ApJ, 144, 886
Sandage, A. 1990, ApJ, 350, 631
Sandage, A., & Hartwick, F. D. A. 1977, AJ, 82, 459
Sandage, A., & Walker, M. F. 1955, AJ, 60, 230
Sandage, A., & Wildey, R. 1967, ApJ, 150, 469
Sarajedini, A. 1992a, AJ, 104, 178
———. 1992b, PhD thesis, Yale University
Sarajedini, A., & Da Costa, G. S. 1991, AJ, 102, 628
Sarajedini, A., & Demarque, P. 1990, ApJ, 365, 219

© American Astronomical Society • Provided by the NASA Astrophysics Data System

1994ApJ...423..248L

Searle, L., & Zinn, R. 1978, ApJ, 225, 357 (SZ)
Seitzer, P., & Carney, B. W. 1990, AJ, 99, 229
Stellingwerf, R. F. 1984, ApJ, 277, 322
Stetson, P. B. 1981, AJ, 86, 687
Stetson, P. B., & Harris, W. E. 1977, AJ, 82, 954
Stetson, P. B., VandenBerg, D. A., Bolte, M. J., Hesser, J. E., & Smith, G. H. 1989, AJ, 97, 1360
Suntzeff, N. 1981, ApJS, 47, 1
Suntzeff, N., Kinman, T. D., & Kraft, R. P. 1991, ApJ, 367, 528
Suntzeff, N., Kraft, R. P., & Kinman, T. D. 1988, AJ, 95, 91
Suntzeff, N., Olszewski, E., & Stetson, P. B. 1985, AJ, 90, 1481
Sweigart, A. V. 1987, ApJS, 65, 95
Sweigart, A. V., & Gross, P. G. 1976, ApJS, 32, 367
Sweigart, A. V., Renzini, A., & Tornambé, A. 1987, ApJ, 312, 762
Tuggle, R. S., & Iben, I. 1972, ApJ, 178, 455
van Albada, T. S., & Baker, N. 1971, ApJ, 169, 311
VandenBerg, D. A. 1983, ApJS, 51, 29
———. 1985, in Production and Distribution of C, N, and O Elements, ed. I. J. Danziger, F. Matteucci, & K. Kjar (Garching: ESO), 73
VandenBerg, D. A., & Bell, R. A. 1985, ApJS, 58, 561
VandenBerg, D. A., Bolte, M. J., & Stetson, P. B. 1990, AJ, 100, 445
van den Bergh, S. 1967, AJ, 72, 70
Yi, S.-Y., Lee, Y.-W., & Demarque, P. 1993, ApJ, 411, L25
Zinn, R. 1980, ApJS, 42, 19
———. 1985, ApJ, 293, 424
Zinn, R. 1986, in Stellar Populations, ed. C. A. Norman, A. Renzini, & M. Tosi (Cambridge Univ. Press), 73
———. 1990, JRASC, 84, 89
Zinn, R., & West, M. J. 1984, ApJS, 55, 45 (ZW)

© American Astronomical Society • Provided by the NASA Astrophysics Data System